A

DISSERTATION

ON

APPLICABILITY OF OCTAHEDRON AS PRO-SILTATION MEASURE AND DETERMINATION OF MOST EFFICIENT PATTERN

Submitted in partial fulfilment of the requirements for the award of the degree of

MASTERS OF TECHNOLOGY

in

CIVIL ENGINEERING

(With Specialization in Water Resources Engineering)

UNDER

ASSAM SCIENCE AND TECHNOLOGY UNIVERSITY

Submitted by:

ROZINA AHMED

MTECH 4th SEMESTER

Roll no- 220620061016

Under the guidance of:

MRS RHITWIKA BARMAN

ASSISTANT PROFESSOR

DEPARTMENT OF CIVIL ENGINEERING

ASSAM ENGINEERING COLLEGE

JALUKBARI, GUWAHAT1-781013

CANDIDATE DECLARATION

I hereby certify that the work presented in the dissertation report entitled " **APPLICABILITY OF OCTAHEDRON AS PRO-SILTATION MEASURE AND DETERMINATION OF MOST EFFICIENT PATTERN** " is accorded for the award of degree of **MASTER OF TECHNOLOGY** with specialisation in water resources engineering, submitted in the department of Civil Engineering, Assam Engineering College, Guwahati, Assam has been carried out by me under the guidance of **MRS RHITWIKA BARMAN**, Assistant Professor, Department of Civil Engineering, Assam Engineering College, Guwahati.

The content of this report have not been submitted to any other university for the award of any degree.

Dated –

Rozina Ahmed

M Tech, 4th Semester

Department of Civil Engineering

Assam Engineering College

CERTIFICATE OF APPROVAL FROM GUIDE

This is to certify that the dissertation report entitled "**APPLICABILITY OF OCTAHEDRON AS PRO-SILTATION MEASURE AND DETERMINATION OF MOST EFFICIENT PATTERN**" is submitted by **ROZINA AHMED**, Roll No **220620061016**, a student of 4th semester in the Department of Civil Engineering, Assam Engineering College, Guwahati in partial fulfilment for the award of degree of **MASTERS OF TECHNOLOGY** in Civil Engineering with specialisation in Water Resources Engineering under **ASSAM SCIENCE AND TECHNOLOGY UNIVERSITY** has been carried out under my guidance.

The content of this report have not been submitted to any other university for the award of any degree.

Dated:

MRS RHITWIKA BARMAN

Assistant Professor

Department of Civil Engineering

Assam Engineering College

CERTIFICATE OF APPROVAL FROM HEAD OF THE DEPARTMENT

This is to certify that the dissertation report entitled "**APPLICABILITY OF OCTAHEDRON AS PRO-SILTATION MEASURE AND DETERMINATION OF MOST EFFICIENT PATTERN**" is submitted by **ROZINA AHMED**, Roll No **220620061016**, a student of 4th semester in the Department of Civil Engineering, Assam Engineering College, Guwahati in partial fulfilment for the award of degree of **MASTERS OF TECHNOLOGY** in Civil Engineering with specialisation in Water Resources Engineering under **ASSAM SCIENCE AND TECHNOLOGY UNIVERSITY** has been carried out and presented in required manner.

The content of this report have not been submitted to any other university for the award of any degree.

Dated:

DR. JAYANTA PATHAK

Professor & Head

Department of Civil Engineering

Assam Engineering College

ACKNOWLEDGEMENT

I would like to express my deep sense of gratitude to all the people whose kind help and guidance has been instrumental towards the completion of this report. I would like to thank my guide **Rhitwika Barman**, Assistant Professor, Department of Civil Engineering, Assam Engineering College for her immense help, kind support and constant encouragement throughout the course of my work.

I am indebted to Dr. Jayanta Pathak, Head of the Department of Civil Engineering and all the faculties of Department of Civil Engineering, Assam Engineering College, for the deep insights and discernment given through the various courses they had taught.

I also like to extend my sincere thanks to the staff of the Department of Civil Engineering at Assam Engineering College, Guwahati. especially the Hydraulics Laboratory where we carried out most of our work. Thank you for the support and opportunities provided.

I also like to thank all my classmates and well-wishers for their constant encouragement, valuable advice and inspiration throughout the work.

Lastly, I acknowledge my indebtedness to all my family members for their whole hearted moral support and constant encouragement.

Date:

Rozina Ahmed

M.Tech, 4th Semester

Department of Civil Engineering

Assam Engineering College

CONTENTS

LIST OF FIGURES

LIST OF TABLES

ABSTRACT

Flooding is a major natural disaster that can cause significant damage to both land and property. One of the most significant problems that occur during floods is the scouring of the river bed and bank, which can lead to a change in the course of the river. To mitigate this problem, a preventive measure called octahedron has been developed.

Permeable model like porcupine, jack jetty are sediment trap system that captures the sediment in the river, thereby controlling scouring. These system have been deployed in large Indian rivers such as the Ganga, Brahmaputra, and Kosi as a cost-effective measure for river training, and has been found to produce positive results in capturing sediment.

In this thesis, an in-depth study of a new sediment trap efficiency system of name Octahedron was introduced which is a modified Jack jetty and different laboratory experiments were Conducted. Using various dimensional parameters, trial octahedron field models were prepared and laid on the channel with the simulated river bed. The research aimed to investigate the sediment deposition pattern for various configurations of octahedron, with specific focus on discharge and sediment concentration of the river. The research findings provide valuable insights into the sediment trap efficiency of octahedron systems and can be used to improve the design and implementation of sediment trap systems in rivers. This can ultimately aid in reducing the impact of floods and protect both land and property.

CHAPTER 1

INTRODUCTION

1.1 General

Rivers with a meandering nature are prone to severe erosion, which can lead to a catastrophic and uncontrollable situation if not properly addressed. This is particularly problematic during the monsoon season, when river erosion accelerates and access to materials and labour becomes limited. To prevent this, it is crucial to take a proactive approach by studying the river's pattern and implementing timely river training measures. These measures can include re-vegetation to reduce flow speed and strategic bank or channel works to stabilize the river channel and protect its banks. By effectively training the river, excessive meandering can be prevented, shifting in its course can be minimized, and navigability can be maintained. Ultimately, the key to successfully combating scour is to act preventatively and make use of effective strategies that address the specific needs of the river.

Protection to the river banks is normally accomplished by a variety of river training works including a marginal embankment or levees, guide banks, guide bunds, groynes or spurs, submerged vanes, cut offs, pitching of banks, pitched islands, sills, closing dykes, and longitudinal dykes. Some of these measures are less expensive than others. Considerations in their use, besides effectiveness, include the cost of construction, environmental impact and aesthetics. Permeable structures tend to be the least expensive to construct. The increasing demand of bank protection work in many reaches of rivers has focused attention on an imperative need to develop cost-effective river training measures. Therefore, application of framed structures has gained importance as a cost effective measure for river management. Bandalling, board fencing, Porcupine, jack-jetty systems and tetrahedral frames are some of these cost-effective methods used for river training.

1.2 OBJECTIVE OF THE STUDY

1. To introduce the modified version of jack jetty named as Octahedron structure as pro siltation measure.
2. To check the efficiency of the Octahedron in a laboratory flume in terms of sediment trapping capacity.
3. To conduct experimental investigation and evaluate the efficiency of the system for various of pattern of octahedron field and different depth of flow.

1.3 OPEN CHANNEL FLOW (OCF)

An open channel is a passage through which liquid flows with a free surface exposed to the atmosphere. This type of flow, known as open channel flow or free surface flow, is driven by the component of gravity and is characterized by a hydrostatic pressure distribution. The free surface of the flow is the boundary between the liquid and the air, which can be either stationary or moving. The pressure within the liquid is always hydrostatic, meaning that it is constant throughout the fluid and is determined by the fluid's density and the force of gravity. An example of open channel flow is depicted in Figure 1.1. This type of flow is essential in many natural and man-made systems, such as rivers, canals, and irrigation channels.

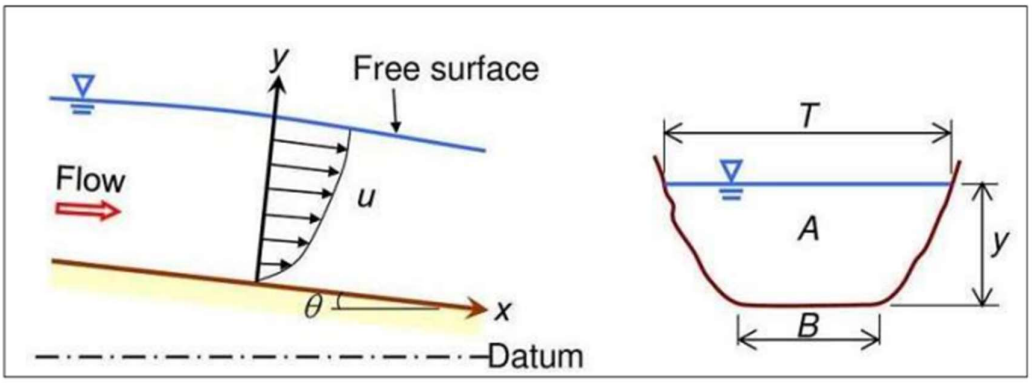

Figure 1.1: Open Channel Flow with hydrostatic pressure distribution.

1.4 MECHANISM OF SEDIMENT TRANSPORT IN OPEN CHANNEL FLOW

Rivers transport sediments in various modes, such as bed load, suspended load, and wash or dissolved load. Bed load sediments move close to the riverbed through rolling, sliding, and hopping, while suspended load sediments move at a large fraction of the mean flow velocity in the stream. Dissolved load, on the other hand, is carried within the water column. The amount of sediments entering the channel greatly influences the channel flow, cross-section and regime. The traditional channel design theory ignored the significance of sediment transport, but it is now acknowledged that a comprehensive study of sediment transport is crucial for successful channel design. Different types of sediment flowing in a channel (figure 1.2) are broadly discussed below.

1. BED LOAD- Bed load is the sediment transported along the riverbed by sliding, rolling, and saltation. It typically makes up 5-20% of total sediment transport and consists of heavy particles such as sand, pebbles, gravels, and cobbles. Saltation is one method of bed load transport in which current lifts sediment from the bed and carries it a certain distance before it falls back to rest. This process can create a chain reaction as particles are lifted and moved, resulting in the exchange of places among similar particles on a non-moving bed.

2. SUSPENDED LOAD- Suspended load is the sediment carried by the flow in suspension, supported by the surrounding fluid, and consisting mostly of smaller particles like clay, silt, and fine sands. It settles when flow velocity decreases. It is kept in suspension by the upward motion due to the turbulence exchange which continuously exchanges fluid over a certain distance between horizontal layers, creating a balance between the settling of sediment and rising fluid from lower layers of higher concentration. Suspended load exerts additional hydrostatic pressure on the riverbed.

3. DISSOLVED LOAD- Dissolved load refers to the particles that are carried in solution by the stream flow. It is a much smaller component of the total sediment transport than suspended and bed load. The dissolved load consists of particles

that are soluble in water and can be derived from the dissolution of rocks in the channel, as well as from tributaries entering the stream.

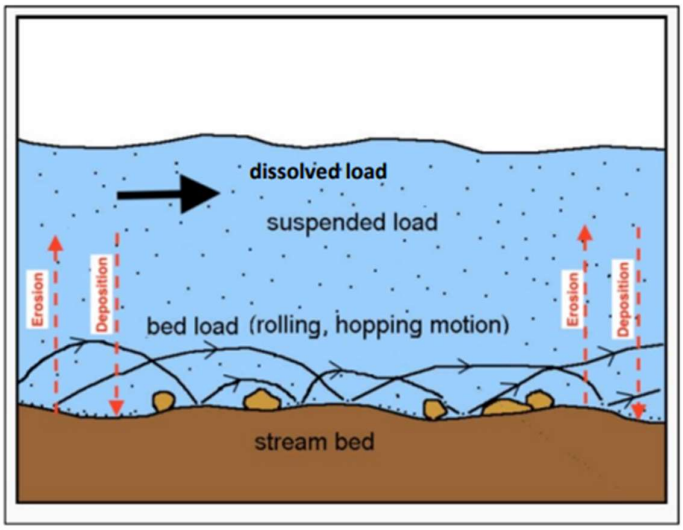

Fig. 1.2: Sediment transport process

1.5 INCIPIENT MOTION CONDITION

The condition of incipient motion of sediment particles refers to the point at which individual particles of a given material begin to move within a fluid flow in an open channel. Determining the exact hydraulic conditions at which this occurs can be challenging, as different criteria can be used to define the point of incipient motion. For example, it could be defined as the point when a single particle starts moving, a few particles start moving, general motion occurs on the bed, or when the rate of sediment transport approaches zero. Despite the difficulty in defining this condition, it is important to understand, as it can have significant implications for the stability of the channel and the behaviour of the sediment particles within the flow.

1.6 RELATED TERMINOLOGY

1.6.1 Erosion

Erosion is the process by which soil, rock, or dissolved material is removed from one location on Earth's crust and transported to another location by the actions of surface processes such as water flow or wind. This process can be further divided into physical or mechanical erosion, in which rock or soil is broken down into elastic sediment, and chemical erosion, where soil or rock is dissolved into a solvent and then transported away. The

transported material can range from a few millimetres to thousands of kilometres away. River Erosion is that in which the river erodes away the bed and banks of its channel vertically and laterally. Vertical erosion is the downward erosion which deepens the river channel. Lateral erosion is sideward erosion which widens the river channel. There are four ways in how the river erode the bed and the bank (EROSIONAL PROCESS)-

(i) Hydraulic Action- The force of river flow helps to break the rock and dragging them away from the bed and the banks of the river.

(ii) Abrasion- The grinding of the rock fragments carried by the river against the banks and bed of the channel. This grinding action will widen and deepen the channel.

(iii) Attrition- The knocking of rock fragments in the water against each other. The fragments are broken into smaller and become smoother pebbles.

(iv) Corrosion- The process in which the water reacts chemically with soluble minerals in the rocks and dissolves them.

1.6.2 Alluvial River

An alluvial river is a type of river characterized by its mobile bed and banks made of sediment and/or soil. These rivers are shaped by the nature and frequency of floods they experience, which shape the channel through erosion, Deposition and sediment transportation. As such, alluvial rivers can take various forms depending on factors such as the properties of the banks, flow patterns, riparian ecology and sediment characteristics.

1.6.3 Properties of Alluvial Rivers

1. Alluvial channels are characterized by their tendency to follow the path of least resistance, resulting in meandering and winding flow patterns.
2. These channels are dynamic, as the loose sedimentary materials can be transported and deposited by water flow, leading to changes in the channel shape and course over time through erosion and sedimentation.

1.7 Jack jetty as river training work

Jack Jetty is a cost-effective river training measure on which study has been carried out through experimental work. Jetty jack which was invented by H. F. Kellner in the early 1920's. This was a permeable form of bank protection and did the job at a lower cost than the non-permeable types of bank protection then in use. He made his first jack with three willow poles tied together at the mid-point. To keep the willow poles extended, he laced them with wire. Afterwards, he replaced the willows with steel angles. Later on modified version of a jack constructed from RCC.

Fig 1.3: Typical RCC Jack jetty on River

Functions: Permeable structures in form of jetty serve one or more of the following functions:

(a) Training the river along the desired course.

(b) Reducing the intensity of flow at the point of river attack.

(c) Creating a slack flow to induce siltation in the vicinity of the permeable structures and in the downstream reach.

(d) Providing protection to the bank by dampening the velocity of flow along the bank.

Use of jack jetty

(a) Can make the river deposit its silt in and around the jack jetty

(b) Can slow down the velocity of flow of the river.

(c) Can stop riverbank erosion.

(d) Can reclaim land i.e., build up scoured or a low area to utilizable level.

(e) Can stop bed scour.

(f) Can maintain bed level.

CHAPTER-2

LITERATURE REVIEW

In recent years, there has been a significant amount of research and investigation on measures to combat siltation and erosion in alluvial rivers such as Ganga, Brahmaputra in India and Jamuna in Bangladesh, using various techniques such as RCC porcupines (both triangular and prismatic), RCC Jack Jetty, submerged vanes, geo bags, and revetments. A comprehensive review of the literature on open channel flow, incipient motion condition, sediment trap efficiency of porcupines, development of a rational design methodology, cost-effective river training structures, and protection of the Majuli island from flood and river bank erosion has been conducted and will be presented in the following paragraphs.

2.1 GENERAL

Sarker et al. (2011) studied that during the last few decades, the Jamuna River has increased its braiding intensity and width. The annual rate of river bank erosion is very high- several thousand hectares per year, which causes millions of people to suffer every year. Satellite images were mainly analyzed to understand the natural bank erosion processes along the right and left sides of the river. Guide bunds, revetment, groynes/spurs were constructed. After that it is seen that the river bank erosion rate continues till date. One part of the reduction is attributed to natural processes while the other is attributed to the bank protection structures, quantification of which is not possible at this moment. The revetment type structures are found to be more stable in the Jamuna River than groyne type structures.

Das (2011) in his book dealt with the concept of open channel flow, analysis of uniform flow, specific energy, force and critical depth computation, hydraulics of alluvial channels, design of channels, steady gradually varied flow, hydraulic jump, rapidly varied flow, spatially varied flow, unsteady flow and dam-break problem.

Punmia et al. (2011) intended to present the currently accepted theories, design principles and practices of soil mechanics and foundation engineering. The book dealt with the elementary properties, soil hydraulics, elasticity applied to soils, compressibility, strength and stability, foundation engineering, pavement design and miscellaneous problems. In addition, twenty-one more common laboratory experiments have been included to illustrate the practice of soil testing.

2.2 INCIPIENT MOTION CONDITION

Garde and Rangaraju (1977) summarized and synthesized the vast amount of information on sediment transport and problems related to alluvial streams scattered in numerous journals, monographs and other research publications. He dealt with the theory of sediment transport and includes and includes such aspects as properties of sediments, incipient motion condition, flow regimes, resistance to flow, bed load transport, suspended load transport and total load transport. He also dealt with applied problems such as sediment samplers and sampling, stable channels, alluvial streams, variations in stream bed elevation and plan forms, sediment control, river training, and miscellaneous problems such as model studies, mud flows, density currents and sediment transport through pipes.

Rijn (1984) presented a method which enables the computation of the suspended load as the depth-integration of the product of the local concentration and flow velocity. The method is based on the computation of the reference concentration from the bed-load transport. Measured concentration profiles have been used for calibration. New relationships are proposed to represent the size gradation of the bed material and the damping of the turbulence by the sediment particles. A verification analysis using about 800 data shows that about 76% of the predicted values are within 0.5 and 2 times the measured values.

Nicholas (2003) examined the potential for investigating flow and suspended sediment transport mechanisms on lowland flood plains using a combination of three-dimensional numerical modelling and acoustic Doppler velocimetry. Model results showed that, contrary to the common perception that suspended sediment transport is controlled predominantly by turbulent mixing processes, horizontal sediment exchanges between the channel and flood plain are largely a product of advection along topographically determined flow lines. Modelled and monitored profiles of time-averaged flow illustrate that vegetative roughness promotes characteristic velocity and turbulent kinetic energy profiles that contrast markedly with the logarithmic "law of the wall". Instantaneous velocity and sediment concentration data obtained at a high sampling frequency confirm that while horizontal sediment transport is dominated by advection, the vertical sediment concentration profile in the lower half of the flow is controlled strongly by the balance between turbulent ejection and sweep events.

Singh and Goswami (2012) examined the impacts of some of the anthropogenic activities that are responsible for the disturbances to the flow and sediment regime as well as to the biogeochemical flux of nutrients through the Brahmaputra River Basin. The study indicated that the erosion and sediment discharge of the river is highly perturbed by human activities and they pose a potential threat to the biogeochemical fluxes of nutrients through the river. Demographic and socio-economic factors considered in this study indicate that the current practices of development and land-use will continue, and these activities will modify the biogeochemical cycles and emissions of key elements in the basin significantly, subsequently contributing strongly to the modification of the global cycles of these elements. In the Brahmaputra River Basin, the ecosystems are formed and changed under the strong forcing of the monsoon climate. Apparently much of the unfavourable change of local ecological climate may be linked to continuing deforestation and increasing land denudation.

2.3 PORCUPINE

Brahmaputra Board, Guwahati (2012) studied that Majuli Island has been under serious attack by the mighty Brahmaputra. Loss of land mass on account of erosion of Brahmaputra River right bank has been regular feature for Majuli Island. Brahmaputra Board prepared a scheme in November 1999 for "Protection of Majuli Island from floods and erosion" at the estimated cost of Rs. 86.56 crores. The work was carried out in three phases- Phase 1 started in March 2005 and was completed in April 2011. Phase 2 and Phase 3 were on progress till 2012. During Phase 1, casting and laying of permeable RCC porcupine screen/spurs/dampeners at various locations were done due to which erosion got arrested substantially in the severely affected reaches. During Phase 2 and 3, casting and laying of 1,27,396 porcupines were done which encouraged heavy siltation. Area of Majuli Island increased from 502.21 sq. km (2004) to 520.21 sq. km (2011). Further remaining protection works, such as completion of 5 spurs, river bank revetment, laying porcupines at vulnerable locations, contemplated under Phase 2 and Phase 3 were targeted to be completed by March 2014.

Aamir and Sharma (2014) studied that porcupine systems have been deployed as a cost-effective measure for river training and have produced good results in capturing sediment. The experiments for their study were carried out in the Outdoor River Engineering laboratory of the Department WRD&M, IIT Roorkee, situated near the Toda Kalyanpur village, Roorkee. The graphs between trap efficiency and PFDI (Porcupine Field Density Index), keeping sediment concentration (q_s)

fixed and different values of PFSI (Porcupine Field Submergence Index), showed that trap efficiency is inversely proportional to submergence and between trap efficiency and PDFI, keeping PFSI fixed and different values of submergence showed that the trap efficiency is directly proportional to sediment concentration. Results showed that densely configured porcupines have greater efficiency in capturing sediment but taking into account economic constraints, a compromise has to be made in between density and cost effectiveness. Also these are very good for low submergence and high sediment concentration.

2.4 JACK JETTY

Grassel (2002) reported that H.F. Kellner founded first jack jetty named "Kellner Jack" in 1920 which was a permeable form of bank protection performed at a lower cost than the non-permeable type. Kellner started his experiments on a small stream neat his home in Topeka, Kansas. The first jack by Kellner was made with three willow poles tied together at the mid-point. He laced them with wire to keep the willow poles extended. Later on he replaced the willow poles with the steel angles. The structural unit of the system called Jack was composed of 4.88 m long 0.1m*0.1m 0.006m steel angles bolted together at their mid-points. Later on Nayan Sharma (2015) used RCC Jack Jetty in the Ganga River at Nakhwa site located at 11 Km. downstream of Varanasi to inhibit stream bank erosion.

Grassel (2002) describes that the Arkanas River saw the first installations of jetty systems by the Albuquerque District of the U.S. Corps of Engineers, with five on the Arkanas and two on the Rio Grande which were completed in the early 1950s. By 1953 seven additional jetty systems were installed on the Rio Grande. Soon after installation of Jetty systems high flows were experienced by two of the completed projects one on the Purgatorie River in Higbee, Colorado and the other on the Arkanas River in Manzanola, Colorado. In the both cases there was no damage to the permeable jetty systems and bank protection was resolved so the efficiency of those systems were verified.

In Kansas, the jetties were installed by the State Highway Department to protect the bridge across the Cimarron River at Sitka. Before the jetty installation in 1950, the bridge abutment washed twice and both times the bridge was extended. After the installation, the Department was able to remove the extension. (Grassel 2002)

In Nebraska, the Santa Fe Railway bridge protection project in 1947 demonstrated how jetties were used to establish a new bank on a curve that matched the natural curve of the river. The project used 980 units of jacks consisting 12.2 m of retards, 550m of double diversion lines and 14 backup retard lines to achieve a new bank. (Grassel 2002)

In Oklahoma, the railroad company in 1942 installed jetty system to achieve a high bank in a deep channel, a deviation from the recommended use of the system for low to moderate height banks. At first, they graded the slope to 1:2 and then placed the jetty system in usual pattern except for tightly spaced retard lines to form a gridiron of resistance. (Grassel 2002)

Grassel (2002) has again said that in New Mexico, the Santa Fe Railroad used jetty system with success from 1936. The embankments situated next to the banks of the Rio Galisteo had been protected by heavy riprap that was consistently washed out during floods. To build up an auxiliary bank a jetty field was installed and later another row of jacks were installed where the attack of the river was directly against the embankment.

SHARMA NAYAN; NAYAK ANUPAMA(2015) done experiment Ganga River of India at Nakhwa Site by using RCC Jack Jetty and Bamboo Submerged Vanes. The right bank of the channel of the Ganga river near Varanasi is a concave bank and was more susceptible to bank erosion during floods thereby constantly reducing inland navigation depth. During dry weather low flow from December to June, the navigation depth was invariably insufficient. The lab and pilot field study deploying modified RCC Jack Jetty supported by bamboo submerged vanes have achieved the following – the secondary left channel was nearly choked diverting the flow to the navigation channel along right bank, and also the ongoing bank erosion along the right bank could be arrested. Evidently the above transformed channel processes resulted in developing and sustaining the desired Inland navigation waterway along the right bank as evidenced from satellite imagery as well as topographical survey. The encouraging outcome of the pilot field study on the large Ganga river warrants re-aplication of the modified cost effective technology in similar other river systems of the world with required fine tuning for specific site condition.

ABHIGYA SHRIWASTAVA, AND NAYAN SHARMAR (2014) done laboratory experiment on jack jetty field of different pattern and found significant reduction in flow velocity due to the presence of submerged jacks which depends on variety of situations such as, reduction in velocity with bigger jacks than smaller ones. Reduction in velocity is pronounced and is more enhanced in the initial stretch which then tapers off to minimize further downstream of the jack. Effect of submergence could be observed. The work also describes that effect is more prominent for when the arrangement of jack jetty field is for 20 degree at angle of incidence of attack then at 30 degree.

CHAPTER 3

METHODOLOGY OF THE EXPERIMENT

3.1 MATERIALS DESCRIPTION

3.1.1 Model

- In this study we have used a modified jack jetty and named it as Octahedron. Normally a typical jack has 6 member which are joint at a single point. In our experiment we have joined the outer point of the typical jack with new members to increase its stability and functions. After joining the outer point the model takes a shape of octahedron as shown bellow.

Fig 3.1: Octahedron made of MS Rod

- The modified Jack models used in this study were created by scaling down to match the dimensions of the laboratory channel.
- The models were constructed using MS Rods, which were 10mm in thickness and inner member were of 10cm in length and outer member were 14 cm in length.
- Figure provides visual representation of such typical models. These models were used as a representation of the actual size jack to study their performance in the laboratory setting, providing a cost-effective and efficient method to study the efficacy of modified Jack Jetty in controlling erosion and facilitating channelization in rivers.

3.1.2 Bed Material

- The laboratory channel used in this study was filled with bed materials collected from the River Brahmaputra, specifically from the Pandu Port of Maligaon, Guwahati, Assam.
- The bed materials were collected, air-dried and then evaluated for particle size distribution, in order to determine the relative percentages of fine and medium-grained sand, as well as fines present in the sample.
- Specific gravity of the sample was determined by using a pycnometer.
- To replicate the natural conditions of the river bed, the simulated river bed in the laboratory channel, which had a depth of 0.49 meters, was prepared by maintaining the same relative percentages of fine and medium sand that were present in the actual river bed material sample collected from the site. This ensured that the laboratory channel closely mimicked the real-world conditions, providing a more accurate representation of the porcupine system's performance in controlling erosion and facilitating channelization in rivers.

3.1.3 Bank Material

- The laboratory channel used in this study was lined with bank materials collected from the River Brahmaputra, specifically from the Pandu Port of Maligaon, Guwahati, Assam.
- This information was used to replicate the natural conditions of the river bank, in order to provide an accurate representation of the performance of various erosion control measures and bank stabilization techniques in the laboratory setting.

3.2 EXPERIMENTAL CHANNEL DESCRIPTION

- All the experiments for this study were conducted in the Hydraulics Laboratory Channel of Assam Engineering College in Guwahati.
- The channel measures 35 meters in length, 1.8 meters in width and 1.275 meters in depth, with a 0.49 meter thickness of sand bed.

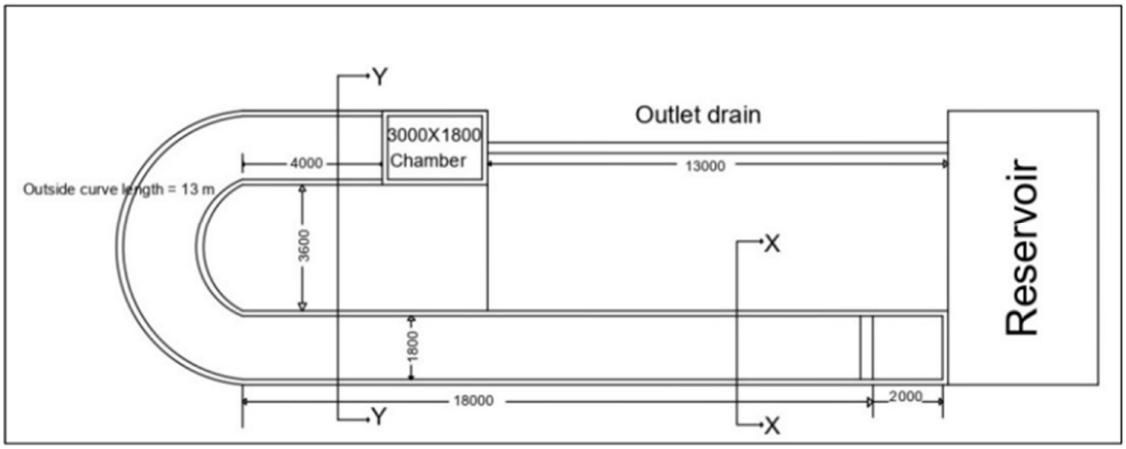

Fig.3.2: Experimental channel

- The water flow in the channel was maintained by utilizing two pumps of5 HP and 10 HP.
- Water from the pumps was collected in a tank, passed through a combined arrangement of energy dissipater and wire mesh screens to reduce turbulence, and then fed into the channel through an inlet.
- The water at the outlet was collected in a rectangular tank and the flow rate into the channel was controlled using a discharge valve at the inlet.

- The slope of the channel bed was taken 1:250 and the slope of the bank was taken as1.5H:1V. This setup provided a controlled environment to study the performance of the erosion control measures and bank stabilization techniques in the laboratory setting.

(A)

(B)

Fig 3.3: Experimental Channel of AEC, Hydraulics Lab

3.3 EXPERIMENTAL PROCEDURE

- The experiments were conducted in the Hydraulics Laboratory Channel of Assam Engineering College in Guwahati. The channel was first levelled and the flow was gradually introduced into it by releasing the discharge valve slowly until reaching the point at which the bed materials just tend to lift, representing incipient motion condition. The valve was then readjusted back a little to maintain a flow velocity less than the critical velocity.
- A clear water run was continued for 45 minutes before starting the experimentation with the Octahedron field models. The rectangular weir was then removed to allow the water to drain out gradually from the channel without disturbing the sand bed. The position of the discharge valve was fixed and kept constant for the rest of the experiments. Sand bed levels were measured with the help of point gauge.
- After placing the first trial model of the Octahedron field, the sediment bed of the channel was again levelled around the field and the flow was introduced. A fixed quantity of sediment was injected into the channel 2 meters upstream of the jack jetty field for 3 hours. The motor was then shut down and the rectangular weir removed to allow the water to drain out gradually from the channel. After the water had completely drained, the sand bed levels were again measured with the help of point gauge.
- The same procedure was followed for the rest of the model Octahedron fields studied in this work.

Figure 3.4: Point Gauge with trolley

3.3.1 Measurement of Velocity

The Acoustic Doppler Velocimeter (ADV) was utilized to accurately measure the velocity of water flow. The Vectrino Velocimeter, a device that utilizes the Doppler Effect, was employed in the ADV. The device emits a short pulse of sound, captures the echo, and then calculates the change in pitch or frequency of the echo to determine the water speed. The Vectrino Velocimeter measures the velocity of water flow in three beam components, parallel to its three beams. The data is reported in both Beam and XYZ coordinate systems. The XYZ coordinates are relative to the probe and are not dependent on the orientation of the Vectrino. In the XYZ coordinate system, a positive velocity in the X-direction is indicated by the arrow on the X-axis. To ensure the accuracy of the measurements, velocity was recorded at three distinct points along the flow path - upstream, midstream, and downstream - for each trial.

Figure 3.5: Acoustic Doppler Velocimeter (ADV)

CHAPTER 4

EXPERIMETAL WORK

4.1 SIEVE ANALYSIS OF BED MATERIAL

The particle size distribution of the bed material was determined as per IS 2720: (Part 4)-1985 using dry sieve analysis.

Table 4.1: Test results of sieve analysis of bed material

Sl. No.	IS Sieve size in mm	Weight retained in gm.	% weight retained	Cumulative % weight retained	% Passing
1	10	0	0	0	100
2	4.75	0	0	0	100
3	2.36	0	0	0	100
4	1.18	20	4	4	96
5	0.60	30	6	10	90
6	0.30	305	61	71	29
7	0.15	135	27	98	2
8	0.075	5	1	99	1
9	Pan	5	1	100	0

Fineness Modulus = $\frac{99}{100}$ = 0.99

The particle size distribution graph is shown in figure 4.1

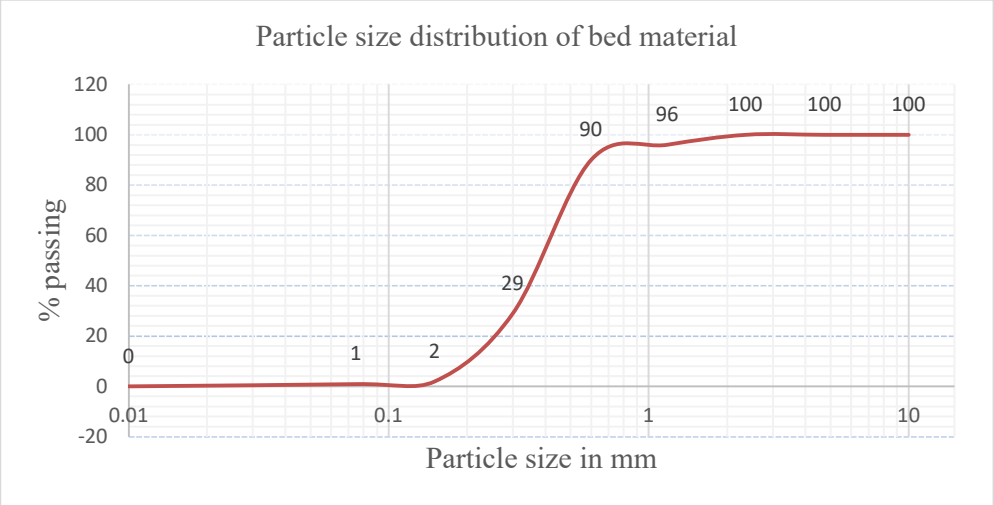

Figure 4.1: Particle size distribution of bed material

From the sieve analysis data, following results were obtained. From the above graph of percentage finer and particle size, the values of D_{10}, D_{30}, D_{50}, D_{60}, C_u and C_c were determined.

Uniformity Coefficient, $C_u = \frac{D_{60}}{D_{10}}$

Coefficient of Curvature, $C_c = (D_{30})^2 / D_{60} \times D_{10}$.

Table 4.2: Summary of particle size distribution of the river bed material

Properties	Value
D_{10} mm	0.22 mm
D_{30} mm	0.4 mm
D_{50} mm	0.43 mm
D_{60} mm	0.49 mm
Uniformity Coefficient, C_u	2.23
Coefficient of Curvature, C_c	1.48
Classification (IS)	Poorly graded sand (SP)

4.2 SIEVE ANALYSIS OF BANK MATERIAL

Table 4.3: Test results of sieve analysis of bank material

Sl. No.	IS Sieve size in mm	Weight retained in gm.	% weight retained	Cumulative % weight retained	% Passing
1	10	0	0	0	100
2	4.75	0	0	0	100
3	2.36	0	0	0	100
4	1.18	0	0	0	100
5	0.60	0	0	0	100
6	0.30	160	32	32	68
7	0.15	205	41	73	27
8	0.075	130	26	99	1
9	Pan	5	1	100	0

Fineness Modulus = $\frac{99}{100}$ = 0.99

The particle size distribution graph is shown in figure 4.2

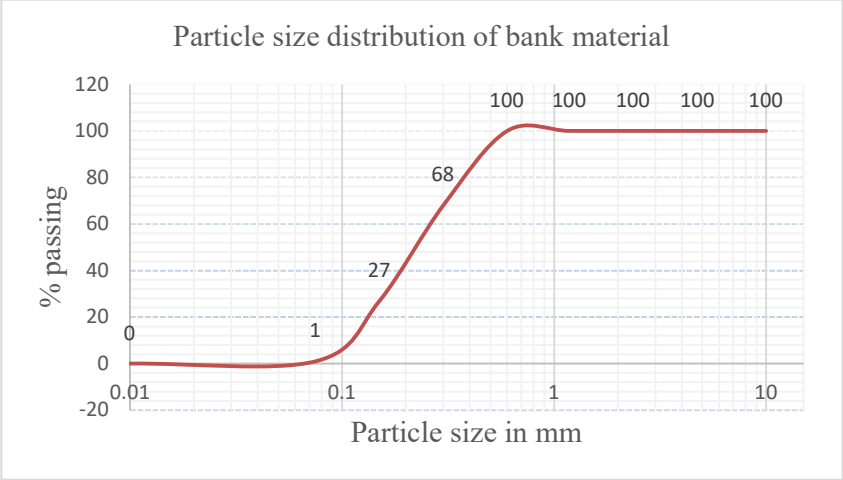

Figure 4.2: Particle size distribution of bank material

From the sieve analysis data, following results were obtained. From the above graph of percentage finer and particle size, the values of D_{10}, D_{30}, D_{50}, D_{60}, C_u and C_c were determined.

Uniformity Coefficient, $C_u = \frac{D_{60}}{D_{10}}$

Coefficient of Curvature, $C_c = (D_{30})^2 / D_{60} \times D_{10}$.

Table 4.4: Summary of particle size distribution of the river bank material

Properties	Value
D_{10} mm	0.22 mm
D_{30} mm	0.19 mm
D_{50} mm	0.25 mm
D_{60} mm	0.29 mm
Uniformity Coefficient, C_u	1.32
Coefficient of Curvature, C_c	0.56
Classification (IS)	Poorly graded sand (SP)

4.3 SPECIFIC GRAVITY OF BED MATERIAL

Specific Gravity (Pycnometer)

Table 4.5: Data and observation sheet for determination of specific gravity of bed material

Serial No.	Specific Gravity
1	2.5
2	2.5
3	2.75

Average G = 2.58

4.4 SPECIFIC GRAVITY OF BANK MATERIAL

Specific Gravity (Pycnometer)

Table 4.6: Data and observation sheet for determination of specific gravity of bank material

Serial No.	Specific Gravity
1	2.5
2	2.5
3	3.33

Average G = 2.78

4.5 POROSITY OF BED MATERIAL

Table 4.7: Data and observation sheet for water content determination of bed material

Serial No.	Void ratio
1	0.51
2	0.51
3	0.52

Average e = 0.51

Porosity, n = $\frac{e}{1+e}$ = 34%

4.6 POROSITY OF BANK MATERIAL

Table 4.8: Data and observation sheet for water content determination of bank material

Serial No.	Void ratio
1	0.54
2	0.53
3	0.54

Average e = 0.54

Porosity, n = $\frac{e}{1+e}$ = 35%

4.7 DIRECT SHEAR TEST

The shear parameters of the river bed material were determined using direct shear test. The plot of shear stress versus shear strain and the plot of maximum shear stress versus normal stress are shown in the figure below.

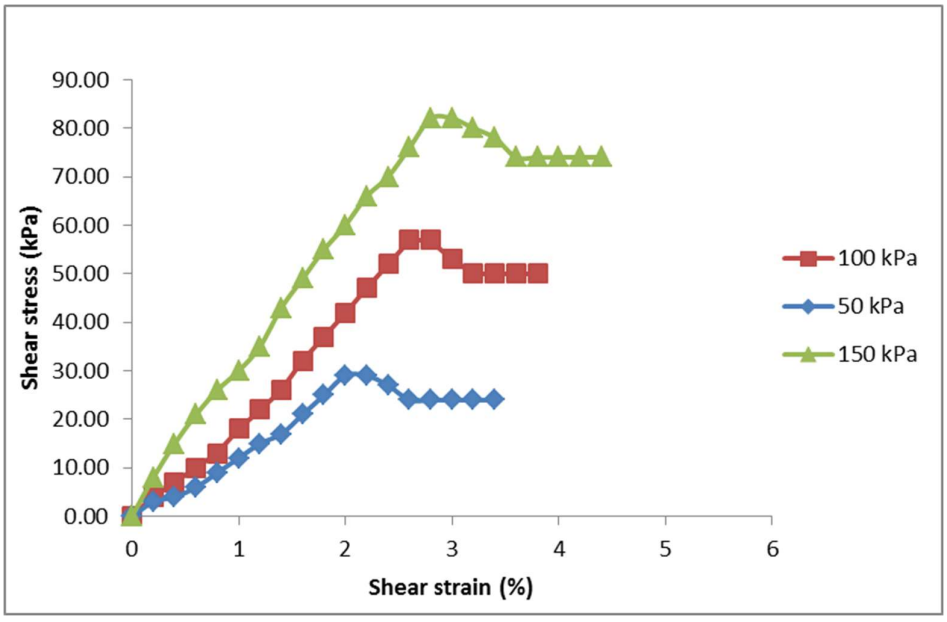

Figure 4.3: Shear stress vs. shear strain at constant shearing rate of 1.25mm/min.

Table 4.9: Maximum shear stress corresponding to each normal stress

Normal stress (kPa)	50	100	150
Maximum shear stress (kPa)	29	57	82

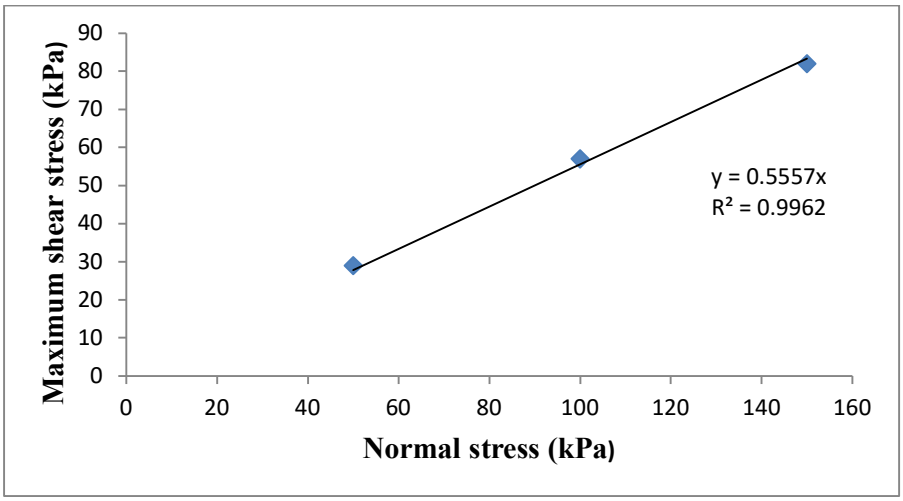

Figure 4.4: Shear stress vs. normal stress graph at shearing rate of 1.25mm/min

$\Phi = 29^{o}$

$C = 0$

4.8 RESULTS OF EXPERIMENTS DONE WITH OCTAHEDRON FIELD MODELS

Trial octahedron field models were prepared and laid on the channel with the simulated river bed. Relevant observations were made to study the sediment deposition of these trial field models as per the methodology laid down and described in the third chapter of this report. After each experimental run, the bed profiles were measured in the form of 0.50 m x 0.50 m grid with point gauge along three imaginary lines (A, B & C) on the channel bed along the flow, as shown in figure 4.5. Figure 4.6 shows typical layout of octahedron field.

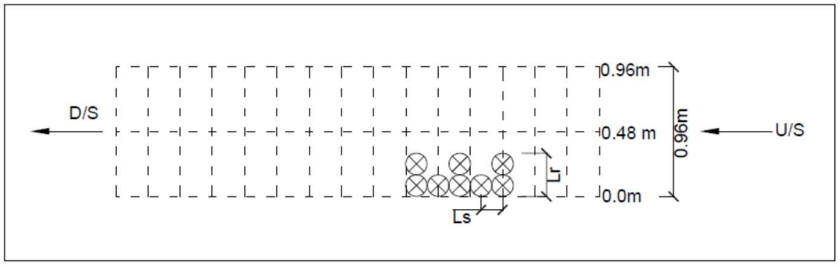

Figure 4.5: Line diagram of channel grid

4.9 INDICES

Some indices were obtained from previous research works which have been calculated for the present study as follows:

A) Octahedron Field Density Index (OFDI) = Length of one retard / Spacing between the two retards = Lr/Ls

B) Octahedron Compartment Density Index (OCDI) = Length of retard / Total length of compartment = Lr/Lc

C) Octahedron Field Length Factor (OFLF) = Length of one compartment of porcupine field / Total length of compartments = Ls/Lc

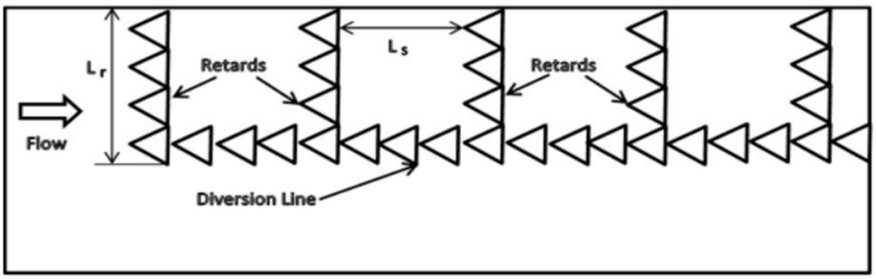

Fig 4.6: Typical layout of model field

(Source: Aamir and Sharma, 2014)

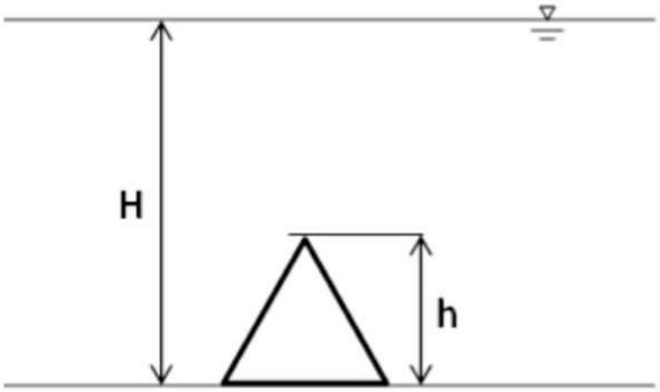

Figure 4.7: Sketch of model submerged in water

(Source: Aamir and Sharma, 2014)

In the present study, a new index has been introduced, known as the Submergence Depth ratio (SDR). It is a ratio between the height of the octahedron and the total depth of water in the channel i.e.

Submergence Depth Ratio (SDR)= Height of octahedron (h) /Total depth of water(H)

Since the height of a Octahedron remains constant for a particular model or set of models, SDR depends on the depth of a water flowing through the channel and are inversely related.

For low depth of flow, SDR>1

For medium depth of flow, SDR<1

For high depth of flow, SDR<<1

Table 4.10: Range of dimensional parameters for the trial octahedron field models

Set No	Arrangement no	Degree of inclination of diversion line to retard	Length of retard	Spacing of retard	Length of compartment	OFLF	OCDI	OFDI
1	1	90	42	15	33	0.454	1.27	2.8
	2	90	42	15	33	0.454	1.27	2.8
2	1	60	43	30	45	0.638	0.957	1.5
	2	90	42	15	33	0.454	1.27	2.8
3	1	45	57.5	15.5	29.5	0.525	1.95	3.5
	2	90	42	15	33	0.454	1.27	2.8

4.10 ESTIMATION OF SEDIMENT DEPOSITION

In this project for a particular type of pattern or arrangement of model we have changed the submergent depth of the field. We have done 3 different submergent depth for one set up. In one set up we have two set of arrangement

4.10.1 first set of Experiments

In the first set of experiment, there are two successive arrangements, one at the inner bank and another at the outer bank each having an angle of inclination of diversion line to the retard as90 degrees. The sediment deposition has been recorded for three depth of flow (low, medium and high).

Table 4.11: Measurement of sediment deposition for low depth of flow (set 1, arrangement 1)

Distance along the length of the channel (m)	Point gauge reading without Octahedron field (m)			Point gauge reading with Octahedron field (m)			Height of ripple of sand (m)		
	A	B	C	A	B	C	A	B	C
0	0.22	0.248	0.224	0.233	0.259	0.229	0.013	0.011	0.005
0.5	0.222	0.245	0.225	0.233	0.254	0.228	0.011	0.009	0.003
1	0.225	0.247	0.225	0.236	0.255	0.23	0.011	0.008	0.005
1.5	0.226	0.246	0.222	0.233	0.252	0.227	0.007	0.006	0.005
2	0.225	0.248	0.221	0.23	0.254	0.224	0.005	0.006	0.003

Figure 4.8: octahedron field for arrangement 1, set1, before experiment, (low depth)

Figure 4.9: Channel bed after experimental run for low depth of flow in Arrangement 1, set 1

Table 4.12: Measurement of sediment deposition for medium depth of flow (set 1, arrangement 1)

Distance along the length of the channel (m)	Point gauge reading without Octahedron field (m)			Point gauge reading with Octahedron field (m)			Height of ripple of sand (m)		
	A	B	C	A	B	C	A	B	C
0	0.233	0.259	0.229	0.256	0.273	0.234	0.023	0.014	0.005
0.5	0.233	0.254	0.228	0.248	0.264	0.235	0.015	0.01	0.007
1	0.236	0.255	0.23	0.247	0.263	0.235	0.011	0.008	0.005
1.5	0.233	0.252	0.227	0.24	0.258	0.232	0.007	0.006	0.005
2	0.23	0.254	0.224	0.235	0.26	0.227	0.005	0.006	0.003

Figure 4.10: octahedron field for arrangement 1, set 1 before experiment, (medium depth)

Figure 4.11: Channel bed after experimental run for medium depth of flow in Arrangement 1, set1

Table 4.13: Measurement of sediment deposition for high depth of flow (set 1, arrangement 1)

Distance along the length of the channel (m)	Point gauge reading without Octahedron field field (m)			Point gauge reading with Octahedron field field (m)			Height of ripple of sand (m)		
	A	B	C	A	B	C	A	B	C
0	0.256	0.273	0.234	0.287	0.284	0.242	0.031	0.011	0.008
0.5	0.248	0.264	0.235	0.269	0.276	0.24	0.021	0.012	0.005
1	0.247	0.263	0.235	0.261	0.271	0.24	0.014	0.008	0.005
1.5	0.24	0.258	0.232	0.247	0.264	0.237	0.007	0.006	0.005
2	0.235	0.26	0.227	0.24	0.266	0.23	0.005	0.006	0.003

Figure 4.12: octahedron field for arrangement 1,set 1 before experiment, (high depth)

Figure 4.13: Channel bed after experimental run for high depth of flow in Arrangement 1, set 1

Table 4.14: Measurement of sediment deposition for low depth of flow (set 1, arrangement 2)

Distance along the length of the channel (m)	Point gauge reading without Octahedron field (m)			Point gauge reading with Octahedron field (m)			Height of ripple of sand (m)		
	A	B	C	A	B	C	A	B	C
0	0.197	0.208	0.198	0.208	0.218	0.204	0.011	0.01	0.006
0.5	0.195	0.205	0.195	0.205	0.214	0.198	0.01	0.009	0.003
1	0.193	0.207	0.185	0.204	0.214	0.19	0.011	0.007	0.005
1.5	0.197	0.206	0.199	0.205	0.211	0.203	0.008	0.005	0.004
2	0.2	0.208	0.201	0.205	0.214	0.204	0.005	0.006	0.003

Figure 4.14: octahedron field for arrangement 2,set 1 before experiment, (low depth)

Figure 4.15: Channel bed after experimental run for low depth of flow in Arrangement 2, set 1

Table 4.15: Measurement of sediment deposition for medium depth of flow (set 1, arrangement 1)

Distance along the length of the channel (m)	Point gauge reading without Octahedron field (m)			Point gauge reading with Octahedron field (m)			Height of ripple of sand (m)		
	A	B	C	A	B	C	A	B	C
0	0.208	0.218	0.204	0.229	0.233	0.209	0.021	0.015	0.005
0.5	0.205	0.214	0.198	0.225	0.225	0.201	0.02	0.011	0.003
1	0.204	0.214	0.19	0.221	0.222	0.195	0.017	0.008	0.005
1.5	0.205	0.211	0.203	0.211	0.215	0.206	0.006	0.004	0.003
2	0.205	0.214	0.204	0.21	0.218	0.207	0.005	0.004	0.003

Figure 4.16: octahedron field for arrangement 2,set 1 before experiment, (medium depth)

Figure 4.17: Channel bed after experimental run for medium depth of flow in Arrangement 2, set1

Table 4.16: Measurement of sediment deposition for high depth of flow (set 1, arrangement 2)

Distance along the length of the channel (m)	Point gauge reading without Octahedron field (m)			Point gauge reading with Octahedron field (m)			Height of ripple of sand (m)		
	A	B	C	A	B	C	A	B	C
0	0.229	0.233	0.209	0.262	0.245	0.218	0.033	0.012	0.009
0.5	0.225	0.225	0.201	0.25	0.234	0.207	0.025	0.009	0.006
1	0.221	0.222	0.195	0.241	0.23	0.2	0.02	0.008	0.005
1.5	0.211	0.215	0.206	0.223	0.221	0.21	0.012	0.006	0.004
2	0.21	0.218	0.207	0.215	0.222	0.21	0.005	0.004	0.003

Figure 4.18: octahedron field for arrangement 2, set 1 before experiment, (High depth)

Figure 4.19: Channel bed after experimental run for high depth of flow in Arrangement 2, set 1

4.10.2 Second set of experiments

In the second set of experiments, there are two successive arrangements, one at the inner bank having 60 degrees inclination of diversion line with retard and another in the outer bank, inclined at 90 degrees to the retard. The sediment deposition has been estimated for three depth of flow (low, medium and high)

Table 4.17: Measurement of sediment deposition for low depth of flow (set2, arrangement 1)

Distance along the length of the channel (m)	Point gauge reading without Octahedron field (m)			Point gauge reading with Octahedron field (m)			Height of ripple of sand (m)		
	At A	At B	At C	At A	At B	At C	At A	At B	At C
0	0.222	0.235	0.237	0.231	0.246	0.253	0.009	0.011	0.016
0.5	0.225	0.23	0.237	0.233	0.242	0.254	0.008	0.012	0.017
1	0.237	0.235	0.234	0.245	0.244	0.245	0.008	0.009	0.011
1.5	0.234	0.243	0.231	0.24	0.25	0.239	0.006	0.007	0.008
2	0.23	0.235	0.225	0.235	0.239	0.231	0.005	0.004	0.006

Figure 4.20: octahedron field for arrangement 1, set2, before experiment, (low depth)

Fig 4.21: Channel bed after experimental run for low depth of flow in Arrangement 1, set 2

Table 4.18: Measurement of sediment deposition for medium depth of flow (set2, arrangement 1)

Distance along the length of the channel (m)	Point gauge reading without Octahedron field (m)			Point gauge reading with Octahedron field (m)			Height of ripple of sand (m)		
	At A	At B	At C	At A	At B	At C	At A	At B	At C
0	0.231	0.246	0.253	0.24	0.259	0.279	0.009	0.013	0.026
0.5	0.233	0.242	0.254	0.241	0.254	0.281	0.008	0.012	0.027
1	0.245	0.244	0.245	0.252	0.253	0.2471	0.007	0.009	0.0021
1.5	0.24	0.25	0.239	0.246	0.257	0.25	0.006	0.007	0.011
2	0.235	0.239	0.231	0.24	0.243	0.237	0.005	0.004	0.006

Figure 4.22: octahedron field for arrangement 1, set2, before experiment, (medium depth)

Figure 4.23: Channel bed after experimental run for medium depth of flow in Arrangement 1, set 2

Table 4.19: Measurement of sediment deposition for high depth of flow (set2, arrangement 1)

Distance along the length of the channel (m)	Point gauge reading without Octahedron field (m)			Point gauge reading with Octahedron field (m)			Height of ripple of sand (m)		
	At A	At B	At C	At A	At B	At C	At A	At B	At C
0	0.24	0.259	0.279	0.25	0.274	0.309	0.01	0.015	0.03
0.5	0.241	0.254	0.281	0.25	0.266	0.312	0.009	0.012	0.031
1	0.252	0.253	0.2471	0.259	0.262	0.2761	0.007	0.009	0.029
1.5	0.246	0.257	0.25	0.252	0.264	0.261	0.006	0.007	0.011
2	0.24	0.243	0.237	0.242	0.247	0.243	0.002	0.004	0.006

Figure 4.24: octahedron field for arrangement 1, set2, before experiment, (high depth)

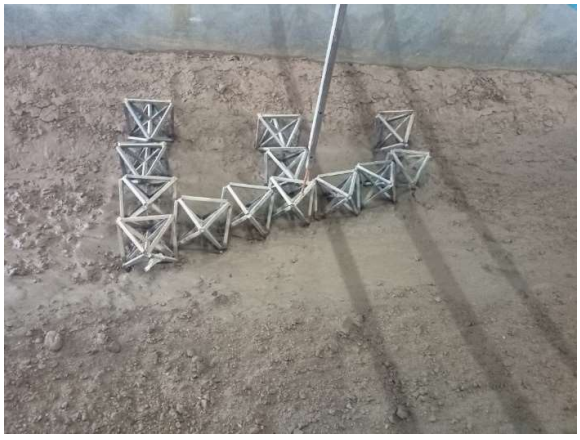

Figure 4.25: Channel bed after experimental run for high depth of flow in Arrangement 1, set 2

Table 4.20: Measurement of sediment deposition for low depth of flow (set2, arrangement 2)

Distance along the length of the channel (m)	Point gauge reading without Octahedron field (m)			Point gauge reading with Octahedron field (m)			Height of ripple of sand (m)		
	At A	At B	At C	At A	At B	At C	At A	At B	At C
0	0.205	0.215	0.21	0.218	0.226	0.219	0.013	0.011	0.009
0.5	0.209	0.21	0.217	0.224	0.222	0.225	0.015	0.012	0.008
1	0.207	0.199	0.214	0.2081	0.208	0.222	0.0011	0.009	0.008
1.5	0.214	0.203	0.211	0.222	0.21	0.217	0.008	0.007	0.006
2	0.213	0.201	0.21	0.219	0.205	0.215	0.006	0.004	0.005

Figure 4.26: octahedron field for arrangement 2, set2, before experiment, (low depth)

Figure 4.27: Channel bed after experimental run for low depth of flow in Arrangement 2, set 2

Table 4.21: Measurement of sediment deposition for medium depth of flow (set2, arrangement 2)

Distance along the length of the channel (m)	Point gauge reading without Octahedron field (m)			Point gauge reading with Octahedron field (m)			Height of ripple of sand (m)		
	At A	At B	At C	At A	At B	At C	At A	At B	At C
0	0.218	0.226	0.219	0.244	0.24	0.228	0.026	0.014	0.009
0.5	0.224	0.222	0.225	0.251	0.234	0.232	0.027	0.012	0.007
1	0.2081	0.208	0.222	0.2102	0.217	0.23	0.0021	0.009	0.008
1.5	0.222	0.21	0.217	0.233	0.217	0.223	0.011	0.007	0.006
2	0.219	0.205	0.215	0.225	0.209	0.22	0.006	0.004	0.005

Figure 4.28: octahedron field for arrangement 2, set2, before experiment, (medium depth)

Figure 4.29: Channel bed after experimental run for medium depth of flow in Arrangement 2, set 2

Table 4.22: Measurement of sediment deposition for high depth of flow (set2, arrangement 2)

Distance along the length of the channel (m)	Point gauge reading without Octahedron field (m)			Point gauge reading with Octahedron field (m)			Height of ripple of sand (m)		
	At A	At B	At C	At A	At B	At C	At A	At B	At C
0	0.244	0.24	0.228	0.274	0.256	0.237	0.03	0.016	0.009
0.5	0.251	0.234	0.232	0.282	0.246	0.242	0.031	0.012	0.01
1	0.2102	0.217	0.23	0.2392	0.226	0.238	0.029	0.009	0.008
1.5	0.233	0.217	0.223	0.244	0.224	0.228	0.011	0.007	0.005
2	0.225	0.209	0.22	0.231	0.213	0.223	0.006	0.004	0.003

Figure 4.30: octahedron field for arrangement 2, set2, before experiment, (high depth)

Figure 4.31: Channel bed after experimental run for high depth of flow in Arrangement 2, set 2

4.10.2 3rd set of experiments

In the 3rd set of experiments, there are two successive arrangements, one at the inner bank having 45 degrees inclination of diversion line with retard and another in the outer bank, inclined at 90 degrees to the retard. The sediment deposition has been estimated for three depths of flow (low, medium and high)

Table 4.23: Measurement of sediment deposition for low depth of flow (set3, arrangement 1)

Distance along the length of the channel (m)	Point gauge reading without Octahedron field (m)			Point gauge reading with Octahedron field (m)			Height of ripple of sand (m)		
	At A	At B	At C	At A	At B	At C	At A	At B	At C
0	0.222	0.235	0.237	0.229	0.246	0.253	0.007	0.011	0.016
0.5	0.225	0.23	0.237	0.233	0.242	0.254	0.008	0.012	0.017
1	0.237	0.235	0.234	0.245	0.244	0.245	0.008	0.009	0.011
1.5	0.234	0.243	0.231	0.24	0.25	0.239	0.006	0.007	0.008
2	0.23	0.235	0.225	0.235	0.239	0.231	0.005	0.004	0.006

Figure 4.32: octahedron field for arrangement 1, set3, before experiment, (low depth)

Figure 4.33: Channel bed after experimental run for low depth of flow in Arrangement 1, set 3

Table 4.24: Measurement of sediment deposition for medium depth of flow (set3, arrangement 1)

Distance along the length of the channel (m)	Point gauge reading without Octahedron field (m)			Point gauge reading with Octahedron field (m)			Height of ripple of sand (m)		
	At A	At B	At C	At A	At B	At C	At A	At B	At C
0	0.229	0.246	0.253	0.238	0.259	0.279	0.009	0.013	0.026
0.5	0.233	0.242	0.254	0.241	0.254	0.281	0.008	0.012	0.027
1	0.245	0.244	0.245	0.252	0.253	0.2471	0.007	0.009	0.0021
1.5	0.24	0.25	0.239	0.246	0.257	0.25	0.006	0.007	0.011
2	0.235	0.239	0.231	0.24	0.243	0.237	0.005	0.004	0.006

Figure 4.34: octahedron field for arrangement 1, set3, before experiment, (medium depth)

Figure 4.35: Channel bed after experimental run for medium depth of flow in Arrangement 1, set 3

Table 4.25: Measurement of sediment deposition for high depth of flow (set3, arrangement 1)

Distance along the length of the channel (m)	Point gauge reading without Octahedron field (m)			Point gauge reading with Octahedron field (m)			Height of ripple of sand (m)		
	At A	At B	At C	At A	At B	At C	At A	At B	At C
0	0.238	0.259	0.279	0.248	0.274	0.309	0.01	0.015	0.03
0.5	0.241	0.254	0.281	0.25	0.266	0.312	0.009	0.012	0.031
1	0.252	0.253	0.2471	0.259	0.262	0.2761	0.007	0.009	0.029
1.5	0.246	0.257	0.25	0.252	0.264	0.261	0.006	0.007	0.011
2	0.24	0.243	0.237	0.242	0.247	0.243	0.002	0.004	0.006

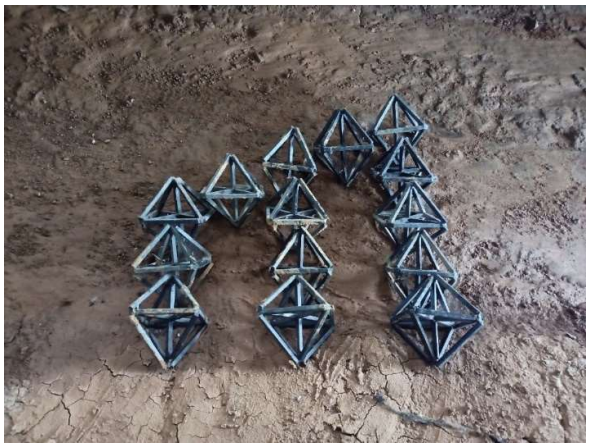

Figure 4.36: octahedron field for arrangement 1, set3, before experiment, (high depth)

Figure 4.37: Channel bed after experimental run for high depth of flow in Arrangement 1, set 3

Table 4.26: Measurement of sediment deposition for low depth of flow (set3, arrangement 2)

Distance along the length of the channel (m)	Point gauge reading without Octahedron field (m)			Point gauge reading with Octahedron field (m)			Height of ripple of sand (m)		
	At A	At B	At C	At A	At B	At C	At A	At B	At C
0	0.205	0.215	0.21	0.218	0.226	0.219	0.013	0.011	0.009
0.5	0.209	0.21	0.217	0.224	0.222	0.225	0.015	0.012	0.008
1	0.207	0.199	0.214	0.2081	0.208	0.222	0.0011	0.009	0.008
1.5	0.214	0.203	0.211	0.222	0.21	0.217	0.008	0.007	0.006
2	0.213	0.201	0.21	0.219	0.205	0.215	0.006	0.004	0.005

Figure 4.38: octahedron field for arrangement 2, set3, before experiment, (low depth)

Figure 4.39: Channel bed after experimental run for low depth of flow in Arrangement 2, set 3

Table 4.27: Measurement of sediment deposition for medium depth of flow (set3, arrangement 2)

Distance along the length of the channel (m)	Point gauge reading without Octahedron field (m)			Point gauge reading with Octahedron field (m)			Height of ripple of sand (m)		
	At A	At B	At C	At A	At B	At C	At A	At B	At C
0	0.218	0.226	0.219	0.244	0.24	0.228	0.026	0.014	0.009
0.5	0.224	0.222	0.225	0.251	0.234	0.232	0.027	0.012	0.007
1	0.2081	0.208	0.222	0.2102	0.217	0.23	0.0021	0.009	0.008
1.5	0.222	0.21	0.217	0.233	0.217	0.223	0.011	0.007	0.006
2	0.219	0.205	0.215	0.225	0.209	0.22	0.006	0.004	0.005

Figure 4.40: octahedron field for arrangement 2, set3, before experiment, (medium depth)

Figure 4.41: Channel bed after experimental run for medium depth of flow in Arrangement 2, set 3

Table 4.28: Measurement of sediment deposition for high depth of flow (set3, arrangement 2)

Distance along the length of the channel (m)	Point gauge reading without Octahedron field (m)			Point gauge reading with Octahedron field (m)			Height of ripple of sand (m)		
	At A	At B	At C	At A	At B	At C	At A	At B	At C
0	0.244	0.24	0.228	0.274	0.256	0.237	0.03	0.016	0.009
0.5	0.251	0.234	0.232	0.282	0.246	0.242	0.031	0.012	0.01
1	0.2102	0.217	0.23	0.2392	0.226	0.238	0.029	0.009	0.008
1.5	0.233	0.217	0.223	0.244	0.224	0.228	0.011	0.007	0.005
2	0.225	0.209	0.22	0.231	0.213	0.223	0.006	0.004	0.003

Figure 4.42: octahedron field for arrangement 2, set3, before experiment, (high depth)

Figure 4.43: Channel bed after experimental run for high depth of flow in Arrangement 2, set 3

4.11 CONTOUR PLOTS OF SEDIMENT LADEN BED

The sediment deposition in the octahedron field with every dimensional variation is shown by contour plots drawn with the help of SURFER software. These plots clearly show the deposition of sand around the octahedron fields.

Length of the octahedron field is indicated starting from the point nearest to the upstream end of channel and width is indicated starting from the wall of the channel. The colour legend shows sediment deposition in m

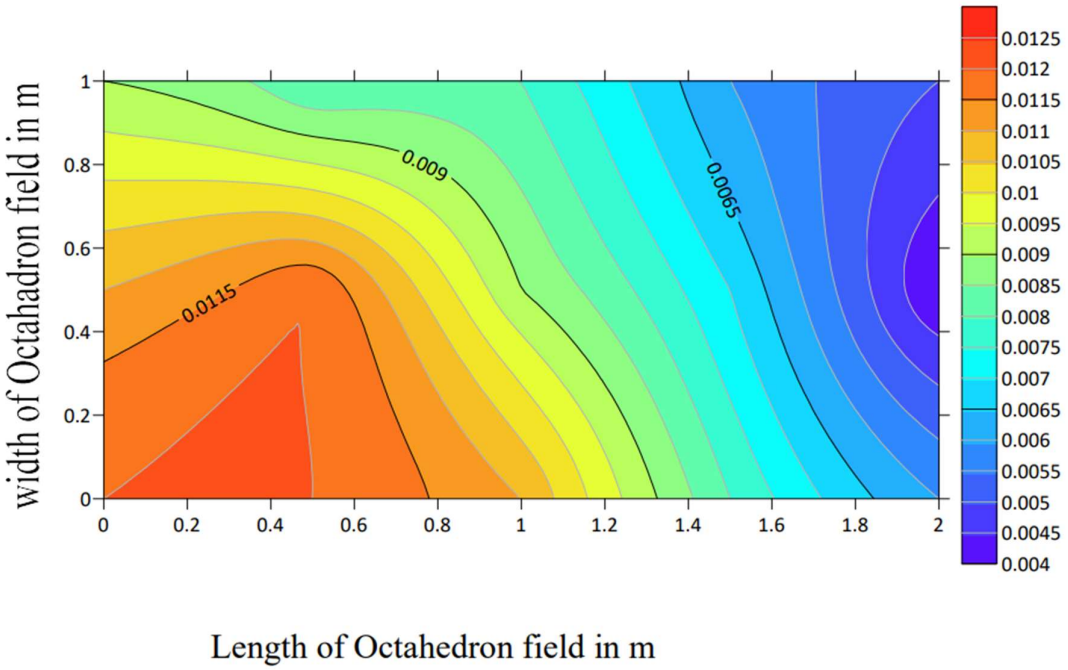

Figure 4.44: Contour plot for set 1, Arrangement 1 of octahedron field (low depth)

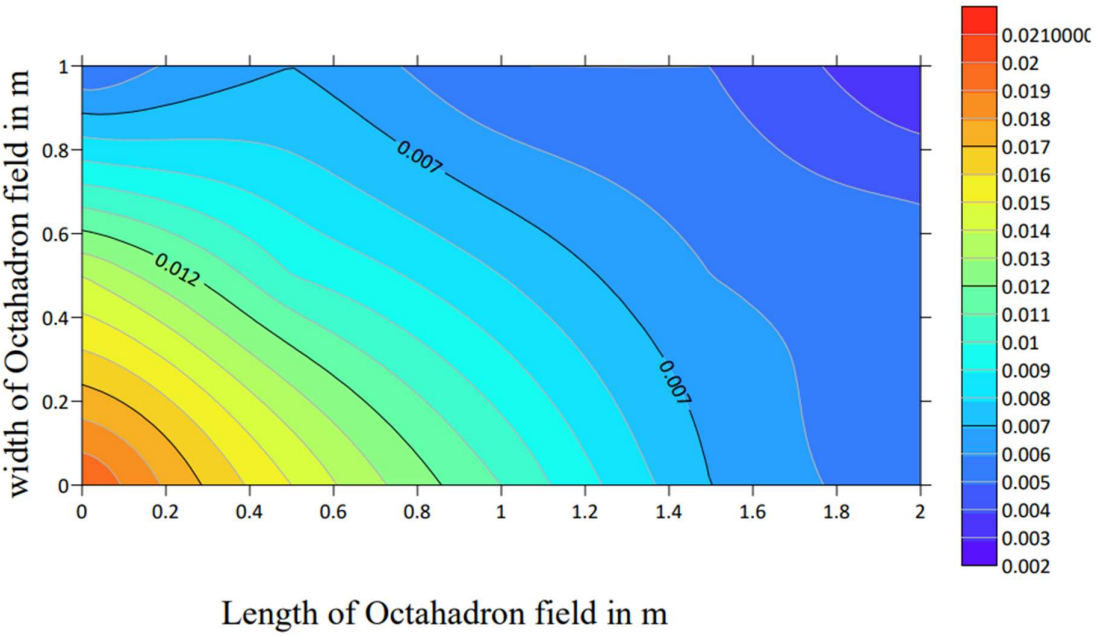

Figure 4.45: Contour plot for set 1, Arrangement 1 of octahedron field (medium depth)

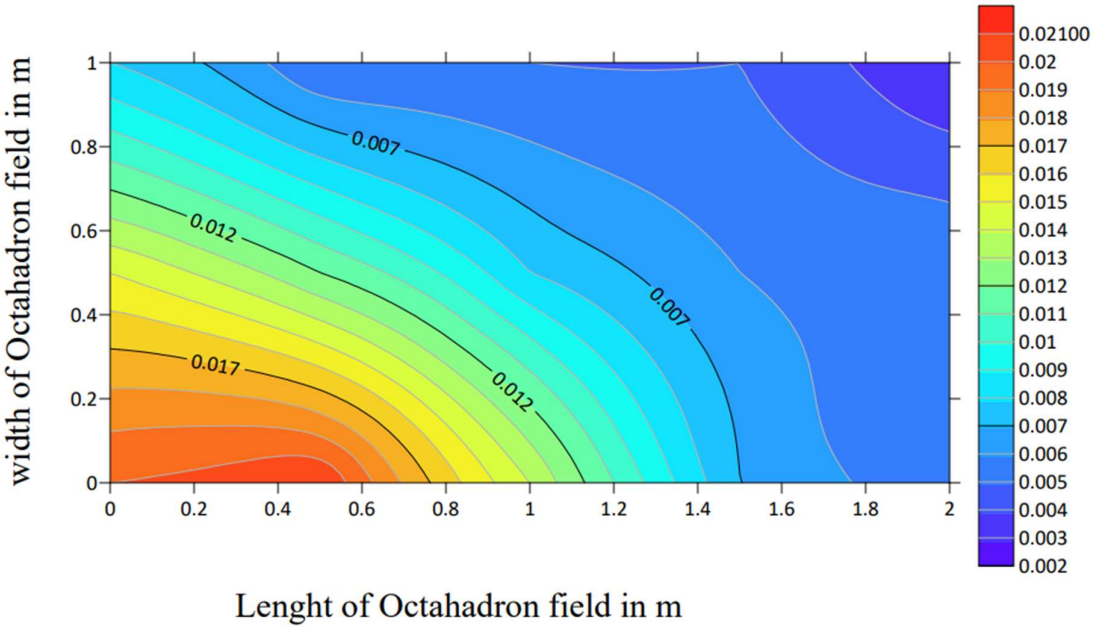

Figure 4.46: Contour plot for set 1, Arrangement 1 of octahedron field (high depth)

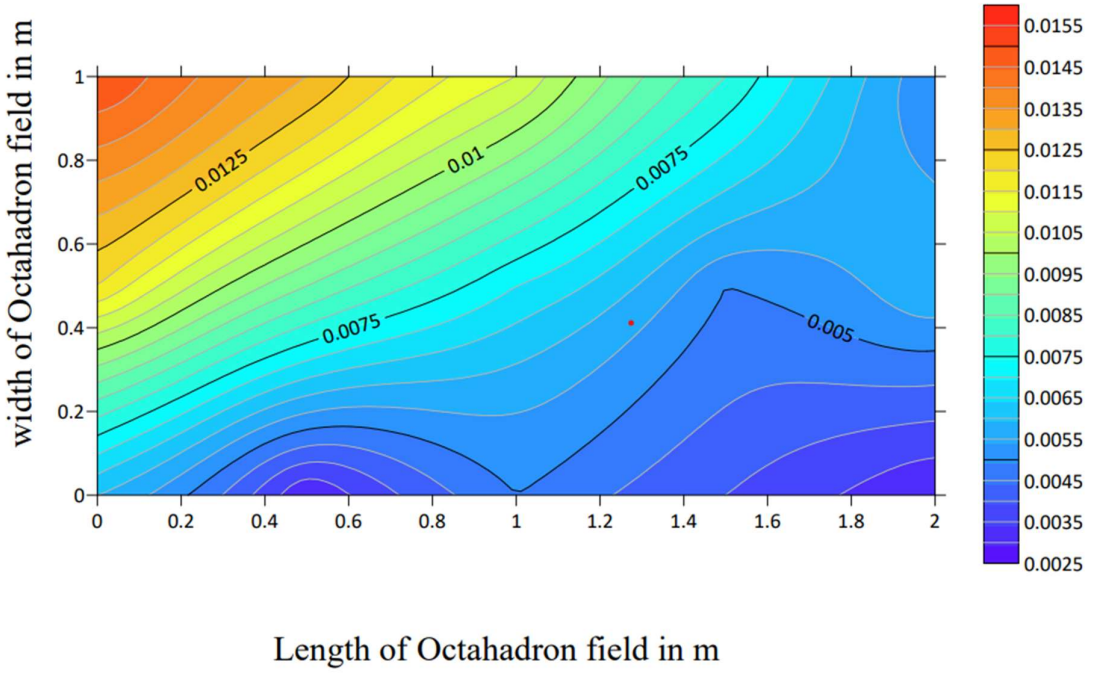

Figure 4.47: Contour plot for set 1, Arrangement 2 of octahedron field (low depth)

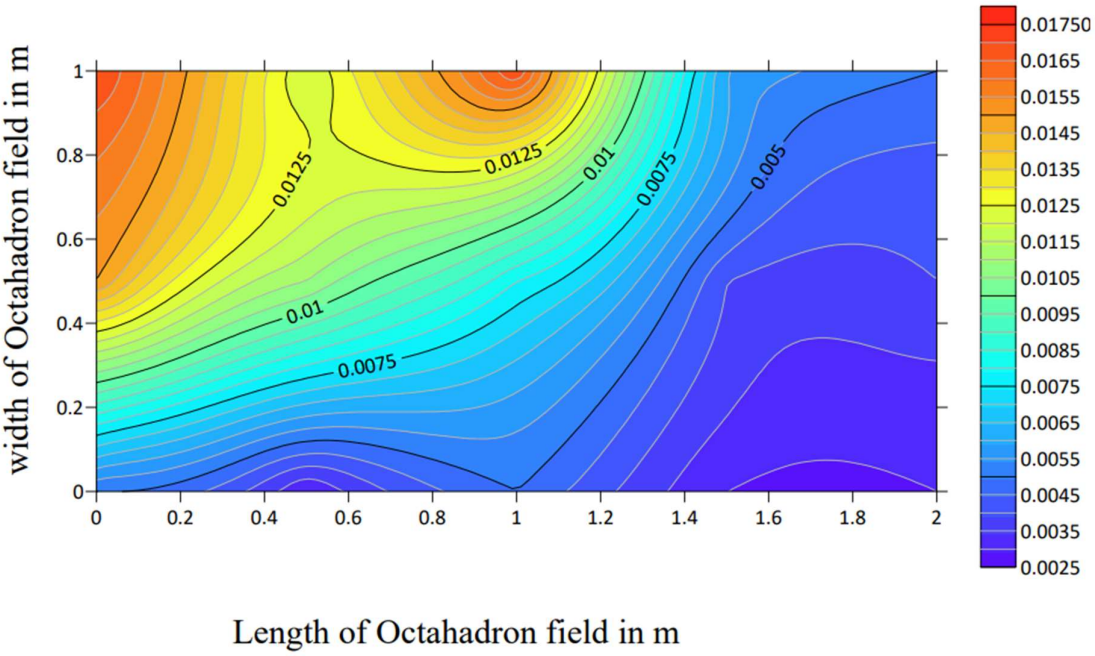

Figure 4.48: Contour plot for set 1, Arrangement 2 of octahedron field (medium depth)

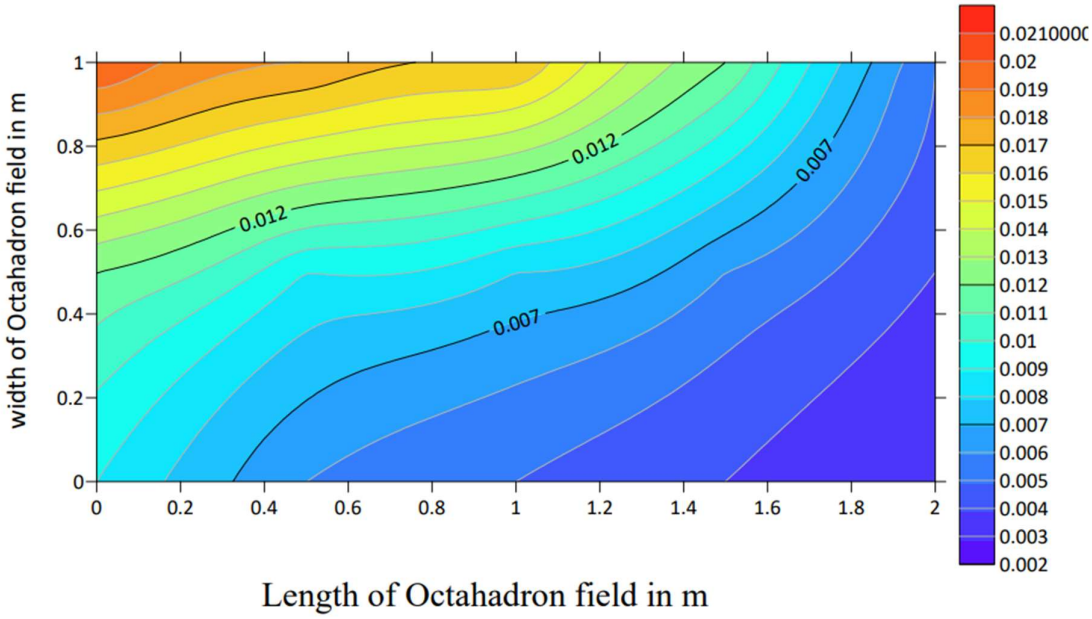

Figure 4.49: Contour plot for set 1, Arrangement 2 of octahedron field (high depth)

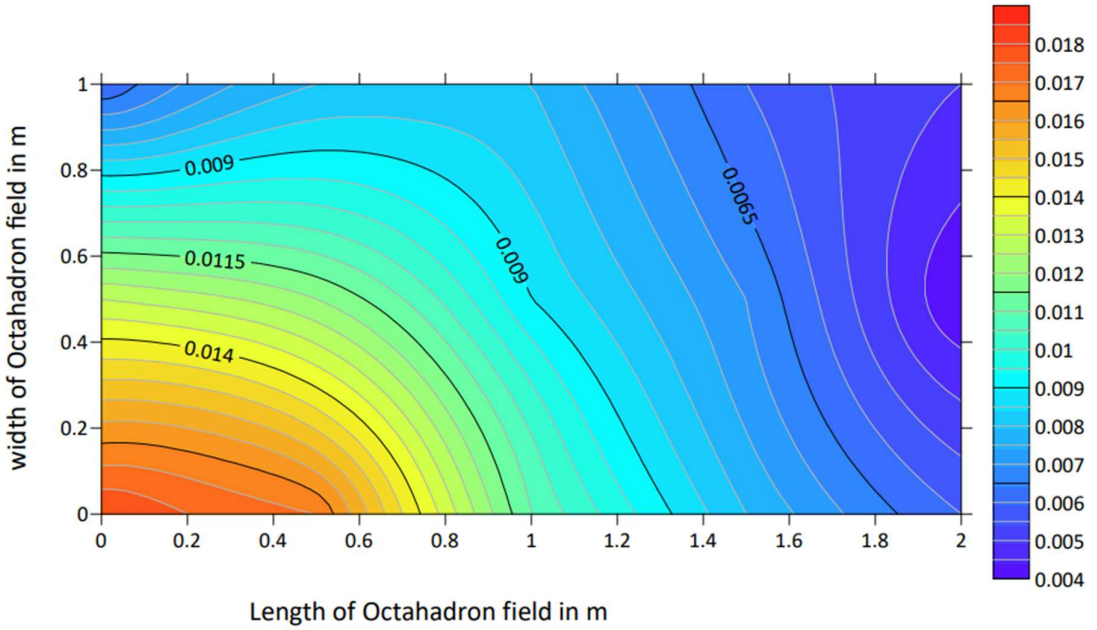

Figure 4.50: Contour plot for set 2, Arrangement 1 of octahedron field (low depth)

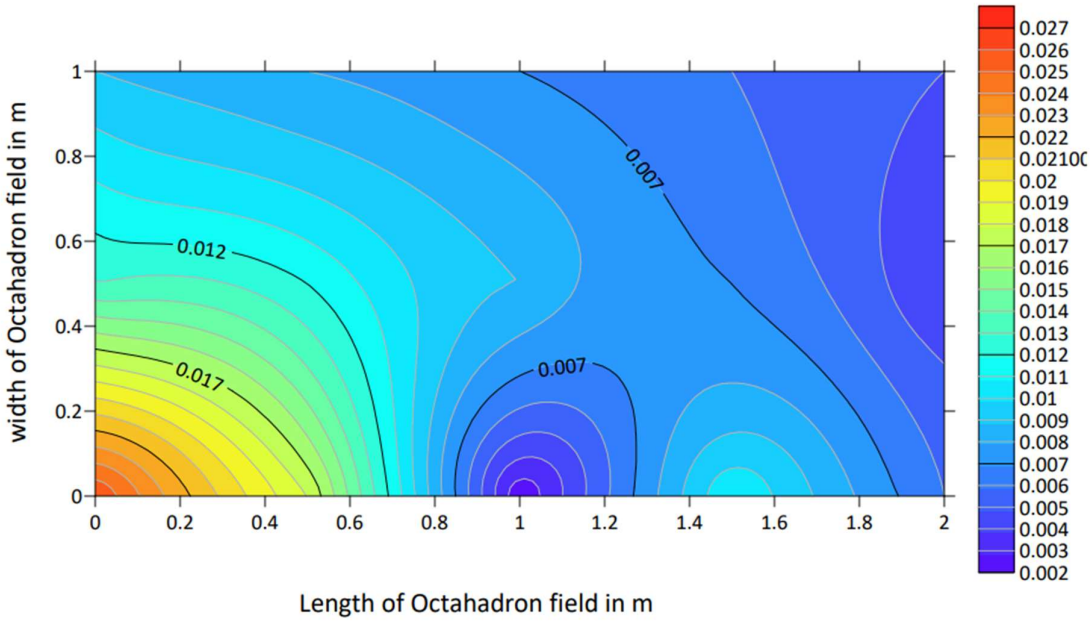

Figure 4.51: Contour plot for set 2, Arrangement 1 of octahedron field (medium depth)

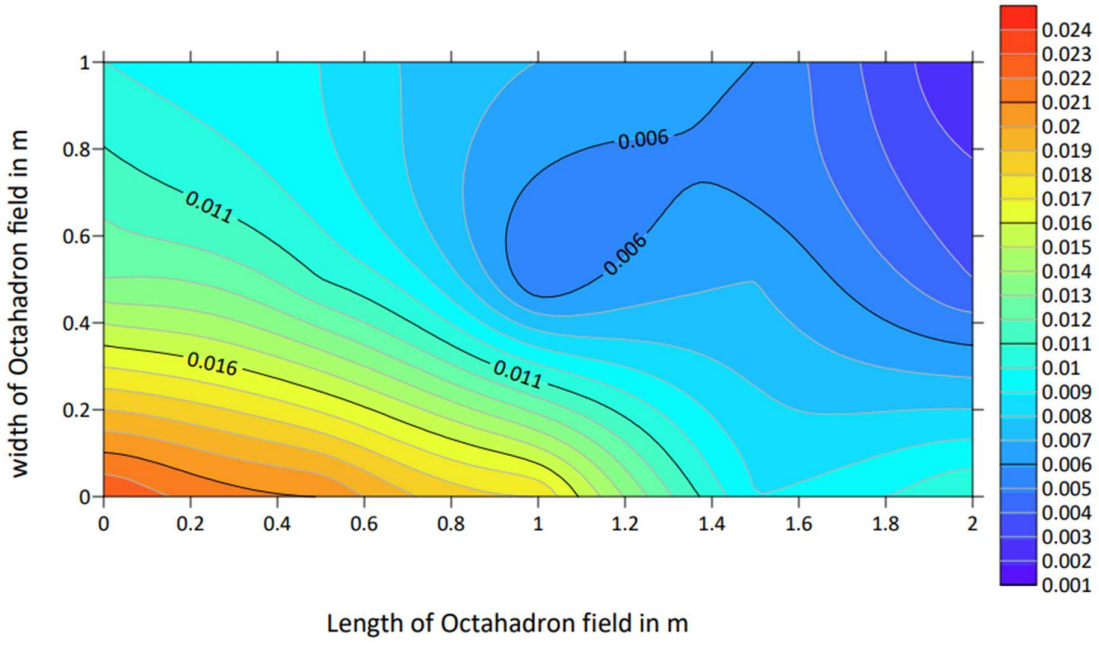

Figure 4.52: Contour plot for set 2, Arrangement 1 of octahedron field (high depth)

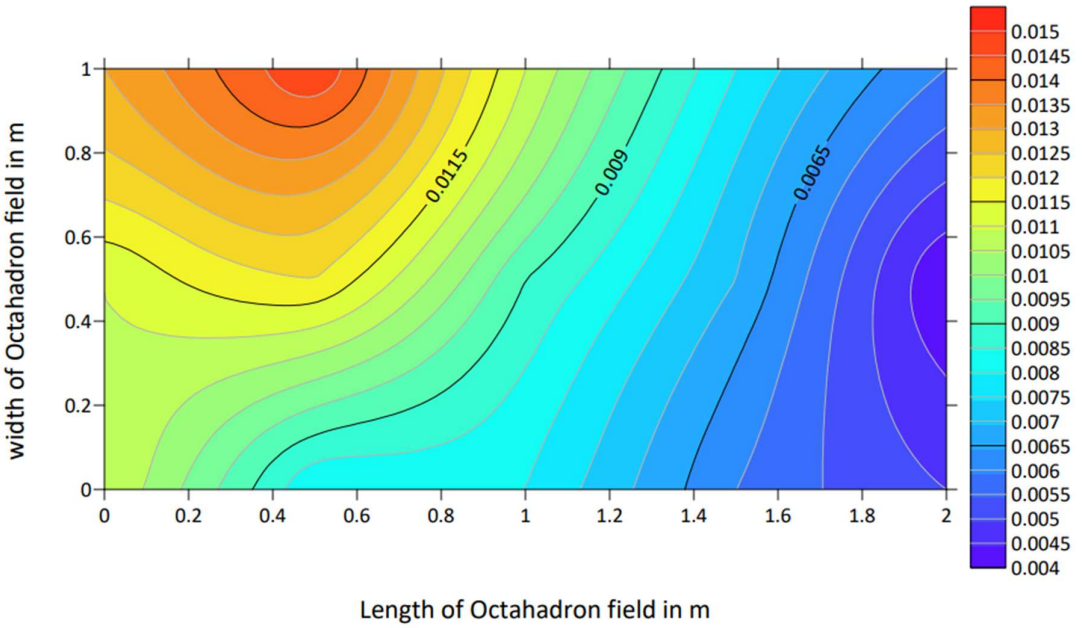

Figure 4.53: Contour plot for set 2, Arrangement 2 of octahedron field (low depth)

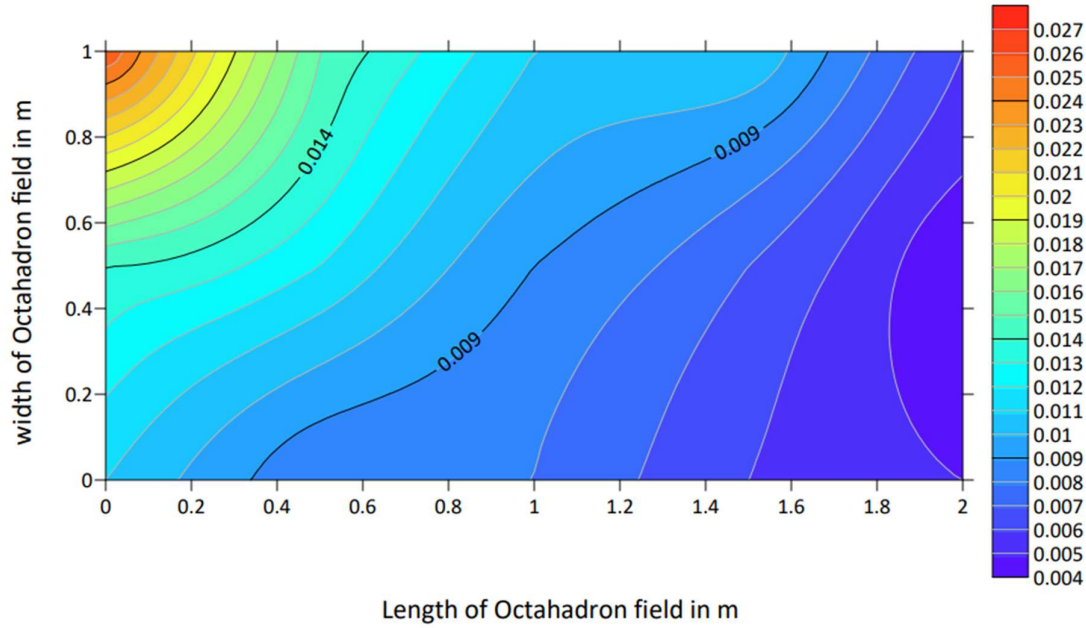

Figure 4.54: Contour plot for set 2, Arrangement 2 of octahedron field (medium depth)

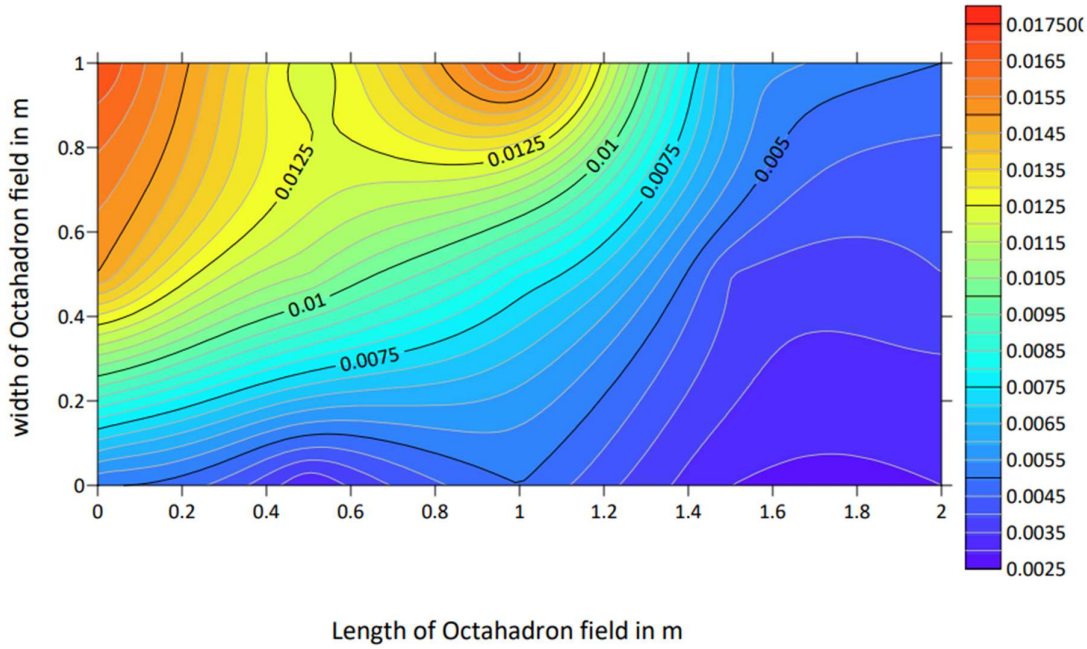

Figure 4.55: Contour plot for set 2, Arrangement 2 of octahedron field (high depth)

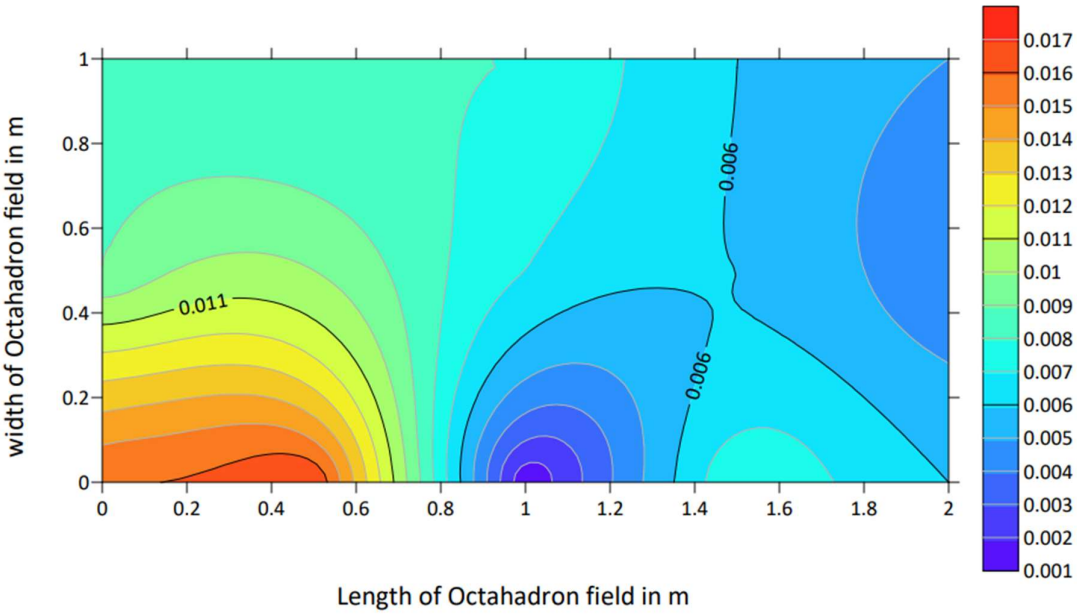

Figure 4.56: Contour plot for set 3, Arrangement 1 of octahedron field (low depth)

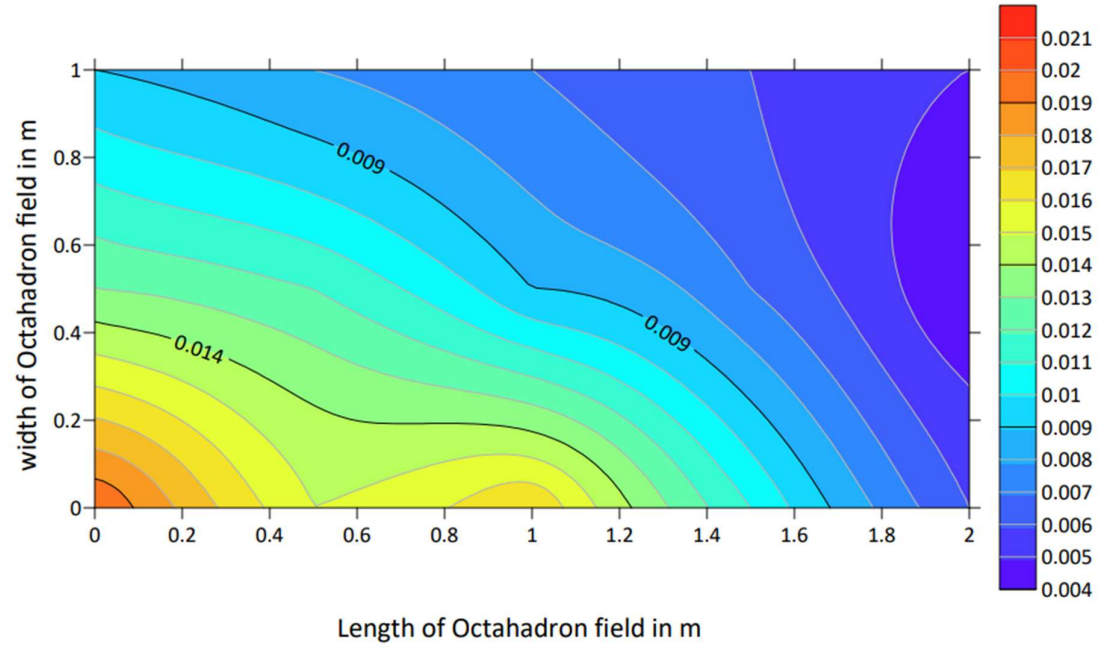

Figure 4.57: Contour plot for set 3, Arrangement 1 of octahedron field (medium depth)

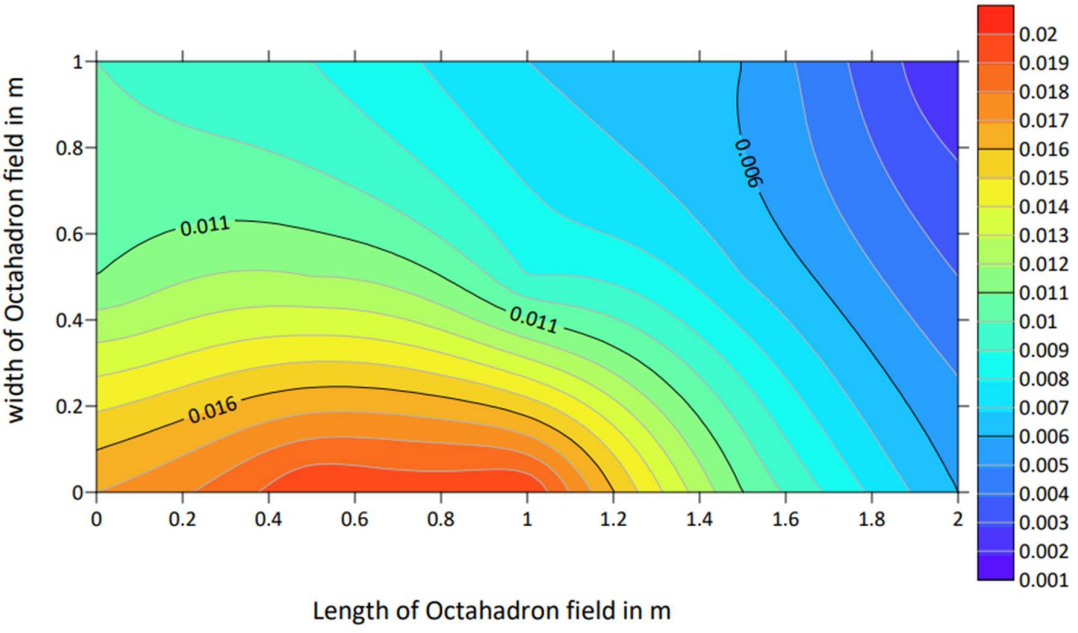

Figure 4.58: Contour plot for set 3, Arrangement 1 of octahedron field (high depth)

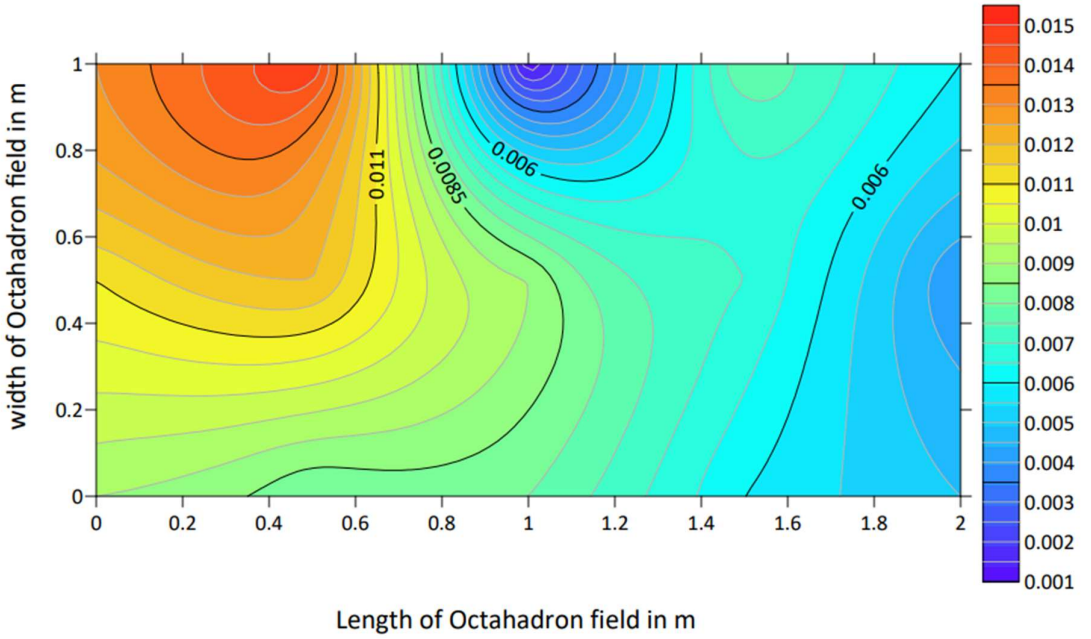

Figure 4.59: Contour plot for set 3, Arrangement 2 of octahedron field (low depth)

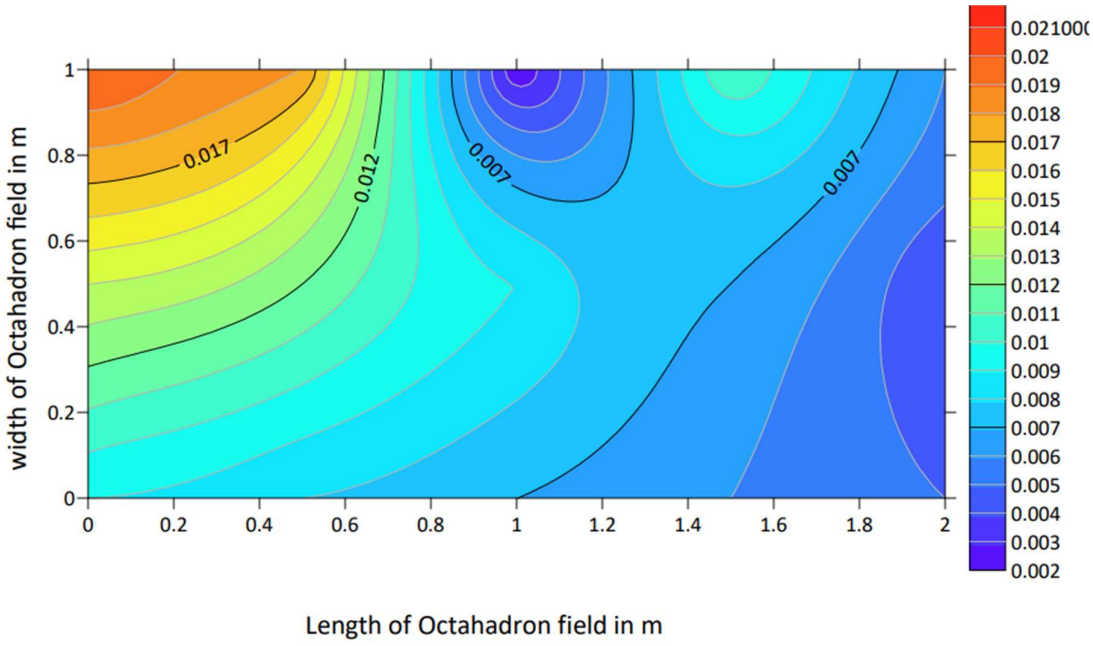

Figure 4.60: Contour plot for set 3, Arrangement 2 of octahedron field (medium depth)

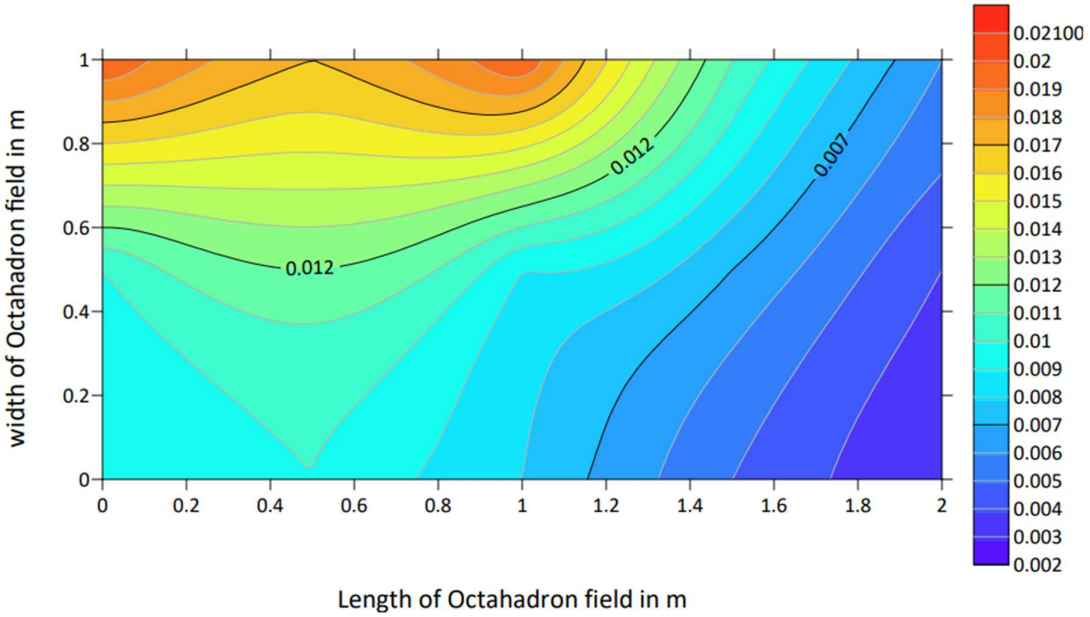

Figure 4.61: Contour plot for set 3, Arrangement 2 of octahedron field (high depth)

4.12 CALCULATION OF SEDIMENT DEPOSITION FOR EACH TRIAL

For Arrangement 1 of set 1 of octahedron field model layout for low depth of flow

Table 4.29: Estimation of sediment deposition in the octahedron field at section A of Arrangement 1 of set 1 for low depth of flow

Distance along the length of the channel (m)	Ripple Height	Radius of Cone (r)	Total Volume of sand	Volume of sand taking porosity into consideration	Weight of sand trapped (kg)
	'h' (m)	in (m)	V= (∏r² h)/3	(m^3)	W= ∂ V'
		r=h/tan Ø		V' = V-35% V	∂ = 2040 Kg/m^3
		Ø= 29°	E=10^		
0	0.009	0.010145	9.70E-07	6.30E-07	1.29E-03
0.5	0.008	0.009018	6.81E-07	4.43E-07	9.03E-04
1	0.008	0.009018	6.81E-07	4.43E-07	9.03E-04
1.5	0.006	0.006763	2.87E-07	1.87E-07	3.81E-04
2	0.005	0.005636	1.66E-07	1.08E-07	2.20E-04
				Total weight	3.69E-03

Table 4.30: Estimation of sediment deposition in the octahedron field at section B of Arrangement 1 of set 1 for low depth of flow

Distance along the length of the channel (m)	Ripple Height	Radius of Cone (r)	Total Volume of sand	Volume of sand taking porosity into consideration	Weight of sand trapped (kg)
	'h' (m)	in (m)	V= (∏r² h)/3	(m^3)	W= ∂ V'
		r=h/tan Ø		V' = V-35% V	∂ = 2040 Kg/m^3
		Ø= 29°	E=10^		
0	0.011	0.0124	1.77E-06	1.15E-06	2.35E-03
0.5	0.012	0.01353	2.30E-06	1.49E-06	3.05E-03
1	0.009	0.01014	9.70E-07	6.30E-07	1.29E-03
1.5	0.007	0.00789	4.56E-07	2.97E-07	6.05E-04
2	0.004	0.00451	8.51E-08	5.53E-08	1.13E-04
				Total weight	7.40E-03

Table 4.31: Estimation of sediment deposition in the octahedron field at section c of Arrangement 1 of set 1 for low depth of flow

Distance along the length of the channel (m)	Ripple Height	Radius of Cone (r)	Total Volume of sand	Volume of sand taking porosity into considerati on	Weight of sand trapped (kg)
	'h' (m)	in (m)	V= (∏r² h)/3	(m³)	W= ∂ V'
		r=h/tan Ø		V' = V- 35% V	∂ = 2040 Kg/m³
		Ø= 29°	E=10^		
0	0.012	0.013527	2.30E-06	1.49E-06	3.05E-03
0.5	0.012	0.013527	2.30E-06	1.49E-06	3.05E-03
1	0.011	0.012399	1.77E-06	1.15E-06	2.35E-03
1.5	0.008	0.009018	6.81E-07	4.43E-07	9.03E-04
2	0.006	0.006763	2.87E-07	1.87E-07	3.81E-04
				Total weight	9.73E-03

Total weight of sand deposited= Sand deposited at A + Sand deposited at B + Sand deposited at C

= (3.69E-03+ 7.40E-03+7.40E-03) kg

= 2.08E-02 Kg

For Arrangement 1 of set 1 of octahedron field model layout for medium depth of flow

Table 4.32: Estimation of sediment deposition in the octahedron field at section A of Arrangement 1 of set 1 for medium depth of flow

Distance along the length of the channel (m)	Ripple Height	Radius of Cone (r)	Total Volume of sand	Volume of sand taking porosity into consideration	Weight of sand trapped (kg)
	'h' (m)	in (m)	V= (∏r² h)/3	(m^3)	W= ∂ V'
		r=h/tan Ø		V' = V-35% V	∂ = 2040 Kg/m^3
		Ø= 29°	E=10^		
0	0.02	0.022544	1.06E-05	6.92E-06	1.41E-02
0.5	0.015	0.016908	4.49E-06	2.92E-06	5.95E-03
1	0.011	0.012399	1.77E-06	1.15E-06	2.35E-03
1.5	0.007	0.00789	4.56E-07	2.97E-07	6.05E-04
2	0.005	0.005636	1.66E-07	1.08E-07	2.20E-04
				Total weight	2.32E-02

Table 4.33 Estimation of sediment deposition in the octahedron field at section B of Arrangement 1 of set 1 for medium depth of flow

Distance along the length of the channel (m)	Ripple Height	Radius of Cone (r)	Total Volume of sand	Volume of sand taking porosity into consideration	Weight of sand trapped (kg)
	'h' (m)	in (m)	$V = (\prod r^2 h)/3$	(m^3)	$W = \partial V'$
		$r = h/\tan Ø$		$V' = V - 35\% V$	$\partial = 2040$ Kg/m^3
		Ø= 29°	E=10^		
0	0.014	0.01578	3.65E-06	2.37E-06	4.84E-03
0.5	0.01	0.01127	1.33E-06	8.64E-07	1.76E-03
1	0.008	0.00902	6.81E-07	4.43E-07	9.03E-04
1.5	0.006	0.00676	2.87E-07	1.87E-07	3.81E-04
2	0.006	0.00676	2.87E-07	1.87E-07	3.81E-04
				Total weight	8.27E-03

Table 4.34: Estimation of sediment deposition in the octahedron field at section C of Arrangement 1 of set 1 for medium depth of flow

Distance along the length of the channel (m)	Ripple Height	Radius of Cone (r)	Total Volume of sand	Volume of sand taking porosity into consideration	Weight of sand trapped (kg)
	'h' (m)	in (m)	V= (∏r² h)/3	(m^3)	W= ∂ V'
		r=h/tan Ø		V' = V-35% V	∂ = 2040 Kg/m^3
		Ø= 29°	E=10^		
0	0.005	0.005636	1.66E-07	1.08E-07	2.20E-04
0.5	0.007	0.00789	4.56E-07	2.97E-07	6.05E-04
1	0.005	0.005636	1.66E-07	1.08E-07	2.20E-04
1.5	0.005	0.005636	1.66E-07	1.08E-07	2.20E-04
2	0.003	0.003382	3.59E-08	2.33E-08	4.76E-05
				Total weight	1.31E-03

Total weight of sand deposited in the 2nd trial= Sand deposited at A + Sand deposited at B + Sand deposited at C

= (2.32E-02+ 8.27E-03– 1.31E-03) kg

= 3.28E-02 kg

For Arrangement 1 of set 1 of octahedron field model layout for high depth of flow

Table 4.35: Estimation of sediment deposition in the octahedron field at section A of Arrangement 1 of set 1 for high depth of flow

Distance along the length of the channel (m)	Ripple Height	Radius of Cone (r)	Total Volume of sand	Volume of sand taking porosity into consideration	Weight of sand trapped (kg)
	'h' (m)	in (m)	V= (∏r² h)/3	(m^3)	W= ∂ V'
		r=h/tan Ø		V' = V-35% V	∂ = 2040 Kg/m^3
		Ø= 29°	E=10^		
0	0.02	0.022544	1.06E-05	6.92E-06	1.41E-02
0.5	0.021	0.023671	1.23E-05	8.01E-06	1.63E-02
1	0.014	0.015781	3.65E-06	2.37E-06	4.84E-03
1.5	0.007	0.00789	4.56E-07	2.97E-07	6.05E-04
2	0.005	0.005636	1.66E-07	1.08E-07	2.20E-04
				Total weight	3.61E-02

Table 4.36: Estimation of sediment deposition in the octahedron field at section B of Arrangement 1 of set 1 for high depth of flow

Distance along the length of the channel (m)	Ripple Height	Radius of Cone (r)	Total Volume of sand	Volume of sand taking porosity into consideration	Weight of sand trapped (kg)
	'h' (m)	in (m)	V= (∏r² h)/3	(m^3)	W= ∂ V'
		r=h/tan Ø		V' = V-35% V	∂ = 2040 Kg/m^3
		Ø= 29°	E=10^		
0	0.015	0.01691	4.49E-06	2.92E-06	5.95E-03
0.5	0.012	0.01353	2.30E-06	1.49E-06	3.05E-03
1	0.008	0.00902	6.81E-07	4.43E-07	9.03E-04
1.5	0.006	0.00676	2.87E-07	1.87E-07	3.81E-04
2	0.006	0.00676	2.87E-07	1.87E-07	3.81E-04
				Total weight	1.07E-02

Table 4.37: Estimation of sediment deposition in the octahedron field at section C of Arrangement 1 of set 1 for high depth of flow

Distance along the length of the channel (m)	Ripple Height	Radius of Cone (r)	Total Volume of sand	Volume of sand taking porosity into consideration	Weight of sand trapped (kg)
	'h' (m)	in (m)	V= (∏r² h)/3	(m^3)	W= ∂ V'
		r=h/tan Ø		V' = V-35% V	∂ = 2040 Kg/m^3
		Ø= 29°	E=10^		
0	0.008	0.009018	6.81E-07	4.43E-07	9.03E-04
0.5	0.005	0.005636	1.66E-07	1.08E-07	2.20E-04
1	0.005	0.005636	1.66E-07	1.08E-07	2.20E-04
1.5	0.005	0.005636	1.66E-07	1.08E-07	2.20E-04
2	0.003	0.003382	3.59E-08	2.33E-08	4.76E-05
				Total weight	1.61E-03

Total weight of sand deposited in the 3rd trial= Sand deposited at A + Sand deposited at B + Sand deposited at C

= (3.61E-02+ 1.07E-02+1.61E-03) kg

= 4.84E-02 kg

For Arrangement 2 of set 1 of octahedron field model layout for low depth of flow

Table 4.38: Estimation of sediment deposition in the octahedron field at section A of Arrangement 2 of set 1 for low depth of flow

Distance along the length of the channel (m)	Ripple Height	Radius of Cone (r)	Total Volume of sand	Volume of sand taking porosity into consideration	Weight of sand trapped (kg)
	'h' (m)	in (m)	V= (∏r² h)/3	(m^3)	W= ∂ V'
		r=h/tan Ø		V' = V-35% V	∂ = 2040 Kg/m^3
		Ø= 29°	E=10^		
0	0.015	0.016908	4.49E-06	2.92E-06	5.95E-03
0.5	0.013	0.014654	2.92E-06	1.90E-06	3.87E-03
1	0.011	0.012399	1.77E-06	1.15E-06	2.35E-03
1.5	0.008	0.009018	6.81E-07	4.43E-07	9.03E-04
2	0.005	0.005636	1.66E-07	1.08E-07	2.20E-04
				Total weight	1.33E-02

Table 4.39: Estimation of sediment deposition in the octahedron field at section B of Arrangement 2 of set 1 for low depth of flow

Distance along the length of the channel (m)	Ripple Height	Radius of Cone (r)	Total Volume of sand	Volume of sand taking porosity into consideration	Weight of sand trapped (kg)
	'h' (m)	in (m)	V= (∏r² h)/3	(m^3)	W= ∂ V'
		r=h/tan Ø		V' = V-35% V	∂ = 2040 Kg/m^3
		Ø= 29°	E=10^		
0	0.012	0.01353	2.30E-06	1.49E-06	3.05E-03
0.5	0.009	0.01014	9.70E-07	6.30E-07	1.29E-03
1	0.007	0.00789	4.56E-07	2.97E-07	6.05E-04
1.5	0.005	0.00564	1.66E-07	1.08E-07	2.20E-04
2	0.006	0.00676	2.87E-07	1.87E-07	3.81E-04
					5.54E-03

Table 4.40: Estimation of sediment deposition in the octahedron field at section C of Arrangement 2 of set 1 for low depth of flow

Distance along the length of the channel (m)	Ripple Height	Radius of Cone (r)	Total Volume of sand	Volume of sand taking porosity into consideration	Weight of sand trapped (kg)
	'h' (m)	in (m)	V= (∏r² h)/3	(m³)	W= ∂ V'
		r=h/tan Ø		V' = V-35% V	∂ = 2040 Kg/m³
		Ø= 29°	E=10^		
0	0.006	0.006763	2.87E-07	1.87E-07	3.81E-04
0.5	0.003	0.003382	3.59E-08	2.33E-08	4.76E-05
1	0.005	0.005636	1.66E-07	1.08E-07	2.20E-04
1.5	0.004	0.004509	8.51E-08	5.53E-08	1.13E-04
2	0.003	0.003382	3.59E-08	2.33E-08	4.76E-05
				Total weight	8.09E-04

Total weight of sand deposited in the 4th trial= Sand deposited at A + Sand deposited at B + Sand deposited at C

= (1.33E-02+ 5.54E-03+ 8.09E-04) kg

= 1.96E-02 kg

For Arrangement 2 of set 1 of octahedron field model layout for medium depth of flow

Table 4.41: Estimation of sediment deposition in the octahedron field at section A of Arrangement 2 of set 1 for medium depth of flow

Distance along the length of the channel (m)	Ripple Height	Radius of Cone (r)	Total Volume of sand	Volume of sand taking porosity into consideration	Weight of sand trapped (kg)
	'h' (m)	in (m)	V= (∏r² h)/3	(m³)	W= ∂ V'
		r=h/tan Ø		V' = V-35% V	∂ = 2040 Kg/m³
		Ø= 29°	E=10^		
0	0.017	0.019163	6.53E-06	4.25E-06	8.66E-03
0.5	0.012	0.013527	2.30E-06	1.49E-06	3.05E-03
1	0.017	0.019163	6.53E-06	4.25E-06	8.66E-03
1.5	0.006	0.006763	2.87E-07	1.87E-07	3.81E-04
2	0.005	0.005636	1.66E-07	1.08E-07	2.20E-04
				Total weight	2.10E-02

Table 4.42: Estimation of sediment deposition in the octahedron field at section B of Arrangement 2 of set 1 for medium depth of flow

Distance along the length of the channel (m)	Ripple Height	Radius of Cone (r)	Total Volume of sand	Volume of sand taking porosity into consideration	Weight of sand trapped (kg)
	'h' (m)	in (m)	V= (∏r² h)/3	(m^3)	W= ∂ V'
		r=h/tan Ø		V' = V-35% V	∂ = 2040 Kg/m^3
		Ø= 29°	E=10^		
0	0.015	0.01691	4.49E-06	2.92E-06	5.95E-03
0.5	0.011	0.0124	1.77E-06	1.15E-06	2.35E-03
1	0.008	0.00902	6.81E-07	4.43E-07	9.03E-04
1.5	0.004	0.00451	8.51E-08	5.53E-08	1.13E-04
2	0.004	0.00451	8.51E-08	5.53E-08	1.13E-04
				Total weight	9.43E-03

Table 4.43: Estimation of sediment deposition in the octahedron field at section C of Arrangement 2 of set 1 for medium depth of flow

Distance along the length of the channel (m)	Ripple Height	Radius of Cone (r)	Total Volume of sand	Volume of sand taking porosity into consideration	Weight of sand trapped (kg)
	'h' (m)	in (m)	V ($\prod r^2$ h)/3	(m^3)	W= ∂ V'
		r=h/tan Ø		V' = V-35% V	∂ = 2040 Kg/m^3
		Ø= 29°	E=10^		
0	0.005	0.005636	1.66E-07	1.08E-07	2.20E-04
0.5	0.003	0.003382	3.59E-08	2.33E-08	4.76E-05
1	0.005	0.005636	1.66E-07	1.08E-07	2.20E-04
1.5	0.003	0.003382	3.59E-08	2.33E-08	4.76E-05
2	0.003	0.003382	3.59E-08	2.33E-08	4.76E-05
				Total weight	5.84E-04

Total weight of sand deposited in the 5th trial= Sand deposited at A + Sand deposited at B + Sand deposited at C

= (2.10E-02+ 9.43E-03+ 5.84E-04) kg

= 3.10E-02 kg

For Arrangement 2 of set 1 of octahedron field model layout for High depth of flow

Table 4.44: Estimation of sediment deposition in the octahedron field at section A of Arrangement 2 of set 1 for high depth of flow

Distance along the length of the channel (m)	Ripple Height	Radius of Cone (r)	Total Volume of sand	Volume of sand taking porosity into consideration	Weight of sand trapped (kg)
	'h' (m)	in (m)	V= (∏r² h)/3	(m^3)	W= ∂ V'
		r=h/tan Ø		V' = V-35% V	∂ = 2040 Kg/m^3
		Ø= 29°	E=10^		
0	0.02	0.022544	1.06E-05	6.92E-06	1.41E-02
0.5	0.018	0.02029	7.76E-06	5.04E-06	1.03E-02
1	0.017	0.019163	6.53E-06	4.25E-06	8.66E-03
1.5	0.012	0.013527	2.30E-06	1.49E-06	3.05E-03
2	0.005	0.005636	1.66E-07	1.08E-07	2.20E-04
				Total weight	3.63E-02

Table 4.45: Estimation of sediment deposition in the octahedron field at section B of Arrangement 2 of set 1 for high depth of flow

Distance along the length of the channel (m)	Ripple Height	Radius of Cone (r)	Total Volume of sand	Volume of sand taking porosity into consideration	Weight of sand trapped (kg)
	'h' (m)	in (m)	V= (∏r² h)/3	(m^3)	W= ∂ V'
		r=h/tan Ø		V' = V-35% V	∂ = 2040 Kg/m^3
		Ø= 29°	E=10^		
0	0.012	0.01353	2.30E-06	1.49E-06	3.05E-03
0.5	0.009	0.01014	9.70E-07	6.30E-07	1.29E-03
1	0.008	0.00902	6.81E-07	4.43E-07	9.03E-04
1.5	0.006	0.00676	2.87E-07	1.87E-07	3.81E-04
2	0.004	0.00451	8.51E-08	5.53E-08	1.13E-04
				Total weight	5.73E-03

Table 4.46: Estimation of sediment deposition in the octahedron field at section C of Arrangement 2 of set 1 for high depth of flow

Distance along the length of the channel (m)	Ripple Height	Radius of Cone (r)	Total Volume of sand	Volume of sand taking porosity into consideration	Weight of sand trapped (kg)
	'h' (m)	in (m)	V= (∏r² h)/3	(m^3)	W= ∂ V'
		r=h/tan Ø		V' = V-35% V	∂ = 2040 Kg/m^3
		Ø= 29°	E=10^		
0	0.009	0.010145	9.70E-07	6.30E-07	1.29E-03
0.5	0.006	0.006763	2.87E-07	1.87E-07	3.81E-04
1	0.005	0.005636	1.66E-07	1.08E-07	2.20E-04
1.5	0.004	0.004509	8.51E-08	5.53E-08	1.13E-04
2	0.003	0.003382	3.59E-08	2.33E-08	4.76E-05
				Total weight	2.05E-03

Total weight of sand deposited in the 6th trial= Sand deposited at A + Sand deposited at B + Sand deposited at C

= (3.63E-02+ 5.73E-03 + 2.05E-03) kg

= 4.41E-02 kg

For Arrangement 1 of set 2 of octahedron field model layout for low depth of flow

Table 4.47: Estimation of sediment deposition in the octahedron field at section A of Arrangement 1 of set 2 for low depth of flow

Distance along the length of the channel (m)	Ripple Height	Radius of Cone (r)	Total Volume of sand	Volume of sand taking porosity into consideration	Weight of sand trapped (kg)
	'h' (m)	in (m)	V= (∏r² h)/3	(m³)	W= ∂ V'
		r=h/tan Ø		V' = V-35% V	∂ = 2040 Kg/m³
		Ø= 29°	E=10^		
0	0.016	0.0180354	5.45E-06	3.54E-06	7.22E-03
0.5	0.017	0.0191626	6.53E-06	4.25E-06	8.66E-03
1	0.011	0.0123994	1.77E-06	1.15E-06	2.35E-03
1.5	0.008	0.0090177	6.81E-07	4.43E-07	9.03E-04
2	0.006	0.0067633	2.87E-07	1.87E-07	3.81E-04
				Total weight	1.95E-02

Table 4.48: Estimation of sediment deposition in the octahedron field at section B of Arrangement 1 of set 2 for low depth of flow

Distance along the length of the channel (m)	Ripple Height	Radius of Cone (r)	Total Volume of sand	Volume of sand taking porosity into consideration	Weight of sand trapped (kg)
	'h' (m)	in (m)	V= (∏r² h)/3	(m³)	W= ∂ V'
		r=h/tan Ø		V' = V-35% V	∂ = 2040 Kg/m³
		Ø= 29°	E=10^		
0	0.011	0.01239936	1.77E-06	1.15E-06	2.35E-03
0.5	0.012	0.01352657	2.30E-06	1.49E-06	3.05E-03
1	0.009	0.01014493	9.70E-07	6.30E-07	1.29E-03
1.5	0.007	0.0078905	4.56E-07	2.97E-07	6.05E-04
2	0.004	0.00450886	8.51E-08	5.53E-08	1.13E-04
				Total weight	7.40E-03

Table 4.49: Estimation of sediment deposition in the octahedron field at section C of Arrangement 1 of set 2 for low depth of flow

Distance along the length of the channel (m)	Ripple Height	Radius of Cone (r)	Total Volume of sand	Volume of sand taking porosity into consideration	Weight of sand trapped (kg)
	'h' (m)	in (m)	V= (∏r² h)/3	(m³)	W= ∂ V'
		r=h/tan Ø		V' = V-35% V	∂ = 2040 Kg/m³
		Ø= 29°	E=10^		
0	0.011	0.012399	1.77E-06	1.15E-06	2.35E-03
0.5	0.008	0.009018	6.81E-07	4.43E-07	9.03E-04
1	0.008	0.009018	6.81E-07	4.43E-07	9.03E-04
1.5	0.006	0.006763	2.87E-07	1.87E-07	3.81E-04
2	0.005	0.005636	1.66E-07	1.08E-07	2.20E-04
				Total weight	4.75E-03

Total weight of sand deposited in the 7th trial= Sand deposited at A + Sand deposited at B + Sand deposited at C

= (1.95E-02+ 7.40E-03+ 4.75E-03) kg

= 3.17E-02 kg

For Arrangement 1 of set 2 of octahedron field model layout for medium depth of flow

Table 4.50: Estimation of sediment deposition in the octahedron field at section A of Arrangement 1 of set 2 for medium depth of flow

Distance along the length of the channel (m)	Ripple Height	Radius of Cone (r)	Total Volume of sand	Volume of sand taking porosity into consideration	Weight of sand trapped (kg)
	'h' (m)	in (m)	V= (∏r² h)/3	(m^3)	W= ∂ V'
		r=h/tan Ø		V' = V-35% V	∂ = 2040 Kg/m^3
		Ø= 29°	E=10^		
0	0.009	0.0101449	9.70E-07	6.30E-07	1.29E-03
0.5	0.008	0.0090177	6.81E-07	4.43E-07	9.03E-04
1	0.007	0.0078905	4.56E-07	2.97E-07	6.05E-04
1.5	0.006	0.0067633	2.87E-07	1.87E-07	3.81E-04
2	0.005	0.0056361	1.66E-07	1.08E-07	2.20E-04
				Total weight	3.39E-03

Table 4.51: Estimation of sediment deposition in the octahedron field at section B of Arrangement 1 of set 2 for medium depth of flow

Distance along the length of the channel (m)	Ripple Height	Radius of Cone (r)	Total Volume of sand	Volume of sand taking porosity into consideration	Weight of sand trapped (kg)
	'h' (m)	in (m)	V=(∏r² h)/3	(m³)	W= ∂ V'
		r=h/tan Ø		V' = V-35% V	∂ = 2040 Kg/m³
		Ø= 29°	E=10^		
0	0.013	0.01465378	2.92E-06	1.90E-06	3.87E-03
0.5	0.012	0.01352657	2.30E-06	1.49E-06	3.05E-03
1	0.009	0.01014493	9.70E-07	6.30E-07	1.29E-03
1.5	0.007	0.0078905	4.56E-07	2.97E-07	6.05E-04
2	0.004	0.00450886	8.51E-08	5.53E-08	1.13E-04
				Total weight	8.92E-03

Table 4.52: Estimation of sediment deposition in the octahedron field at section C of Arrangement 1 of set 2 for medium depth of flow

Distance along the length of the channel (m)	Ripple Height	Radius of Cone (r)	Total Volume of sand	Volume of sand taking porosity into consideration	Weight of sand trapped (kg)
	'h' (m)	in (m)	V= (∏r² h)/3	(m^3)	W= ∂ V'
		r=h/tan Ø		V' = V-35% V	∂ = 2040 Kg/m^3
		Ø= 29°	E=10^		
0	0.026	0.029308	2.34E-05	1.52E-05	3.10E-02
0.5	0.018	0.02029	7.76E-06	5.04E-06	1.03E-02
1	0.0021	0.002367	1.23E-08	8.01E-09	1.63E-05
1.5	0.011	0.012399	1.77E-06	1.15E-06	2.35E-03
2	0.006	0.006763	2.87E-07	1.87E-07	3.81E-04
				Total weight	4.40E-02

Total weight of sand deposited in the 8th trial= Sand deposited at A + Sand deposited at B + Sand deposited at C

= (3.39E-03+ 8.92E-03+ 4.40E-02) kg

= 5.63E-02 kg

For Arrangement 1 of set 2 of octahedron field model layout for High depth of flow

Table 4.53: Estimation of sediment deposition in the octahedron field at section A of Arrangement 1 of set 2 for high depth of flow

Distance along the length of the channel (m)	Ripple Height	Radius of Cone (r)	Total Volume of sand	Volume of sand taking porosity into consideration	Weight of sand trapped (kg)
	'h' (m)	in (m)	V= (∏r² h)/3	(m^3)	W= ∂ V'
		r=h/tan Ø		V' = V-35% V	∂ = 2040 Kg/m^3
		Ø= 29°	E=10^		
0	0.01	0.0112721	1.33E-06	8.64E-07	1.76E-03
0.5	0.009	0.0101449	9.70E-07	6.30E-07	1.29E-03
1	0.007	0.0078905	4.56E-07	2.97E-07	6.05E-04
1.5	0.006	0.0067633	2.87E-07	1.87E-07	3.81E-04
2	0.002	0.0022544	1.06E-08	6.92E-09	1.41E-05
				Total weight	4.05E-03

Table 4.54: Estimation of sediment deposition in the octahedron field at section B of Arrangement 1 of set 2 for high depth of flow

Distance along the length of the channel (m)	Ripple Height	Radius of Cone (r)	Total Volume of sand	Volume of sand taking porosity into consideration	Weight of sand trapped (kg)
	'h' (m)	in (m)	V= (∏r² h)/3	(m^3)	W= ∂ V'
		r=h/tan Ø		V' = V-35% V	∂ = 2040 Kg/m^3
		Ø= 29°	E=10^		
0	0.009	0.01014493	9.70E-07	6.30E-07	1.29E-03
0.5	0.008	0.00901771	6.81E-07	4.43E-07	9.03E-04
1	0.005	0.00563607	1.66E-07	1.08E-07	2.20E-04
1.5	0.007	0.0078905	4.56E-07	2.97E-07	6.05E-04
2	0.004	0.00450886	8.51E-08	5.53E-08	1.13E-04
				Total weight	3.13E-03

Table 4.55: Estimation of sediment deposition in the octahedron field at section B of Arrangement 1 of set 3 for high depth of flow

Distance along the length of the channel (m)	Ripple Height	Radius of Cone (r)	Total Volume of sand	Volume of sand taking porosity into consideration	Weight of sand trapped (kg)
	'h' (m)	in (m)	V= (∏r² h)/3	(m^3)	W= ∂ V'
		r=h/tan Ø		V' = V-35% V	∂ = 2040 Kg/m^3
		Ø= 29°	E=10^		
0	0.011	0.012399	1.77E-06	1.15E-06	2.35E-03
0.5	0.012	0.013527	2.30E-06	1.49E-06	3.05E-03
1	0.03	0.033816	3.59E-05	2.33E-05	4.76E-02
1.5	0.009	0.010145	9.70E-07	6.30E-07	1.29E-03
2	0.006	0.006763	2.87E-07	1.87E-07	3.81E-04
				Total weight	5.47E-02

Total weight of sand deposited in the 9th trial= Sand deposited at A + Sand deposited at B + Sand deposited at C

= (4.05E-03+ 3.13E-03+ 3.81E-02) kg

= 6.18E-02 kg

For Arrangement 2 of set 2 of octahedron field model layout for low depth of flow

Table 4.56: Estimation of sediment deposition in the octahedron field at section A of Arrangement 2 of set 2 for low depth of flow

Distance along the length of the channel (m)	Ripple Height	Radius of Cone (r)	Total Volume of sand	Volume of sand taking porosity into consideration	Weight of sand trapped (kg)
	'h' (m)	in (m)	V= (∏r² h)/3	(m^3)	W= ∂ V'
		r=h/tan Ø		V' = V-35% V	∂ = 2040 Kg/m^3
		Ø= 29°	E=10^		
0	0.013	0.0146538	2.92E-06	1.90E-06	3.87E-03
0.5	0.015	0.0169082	4.49E-06	2.92E-06	5.95E-03
1	0.011	0.0123994	1.77E-06	1.15E-06	2.35E-03
1.5	0.008	0.0090177	6.81E-07	4.43E-07	9.03E-04
2	0.006	0.0067633	2.87E-07	1.87E-07	3.81E-04
				Total weight	1.35E-02

Table 4.57: Estimation of sediment deposition in the octahedron field at section B of Arrangement 2 of set 2 for low depth of flow

Distance along the length of the channel (m)	Ripple Height	Radius of Cone (r)	Total Volume of sand	Volume of sand taking porosity into consideration	Weight of sand trapped (kg)
	'h' (m)	in (m)	V= (∏r² h)/3	(m^3)	W= ∂ V'
		r=h/tan Ø		V' = V-35% V	∂ = 2040 Kg/m^3
		Ø= 29°	E=10^		
0	0.011	0.01239936	1.77E-06	1.15E-06	2.35E-03
0.5	0.012	0.01352657	2.30E-06	1.49E-06	3.05E-03
1	0.009	0.01014493	9.70E-07	6.30E-07	1.29E-03
1.5	0.007	0.0078905	4.56E-07	2.97E-07	6.05E-04
2	0.004	0.00450886	8.51E-08	5.53E-08	1.13E-04
				Total weight	7.40E-03

Table 4.58: Estimation of sediment deposition in the octahedron field at section C of Arrangement 2 of set 2 for low depth of flow

Distance along the length of the channel (m)	Ripple Height	Radius of Cone (r)	Total Volume of sand	Volume of sand taking porosity into consideration	Weight of sand trapped (kg)
	'h' (m)	in (m)	V= (∏r² h)/3	(m³)	W= ∂ V'
		r=h/tan Ø		V' = V-35% V	∂ = 2040 Kg/m³
		Ø= 29°	E=10^		
0	0.011	0.012399	1.77E-06	1.15E-06	2.35E-03
0.5	0.008	0.009018	6.81E-07	4.43E-07	9.03E-04
1	0.008	0.009018	6.81E-07	4.43E-07	9.03E-04
1.5	0.006	0.006763	2.87E-07	1.87E-07	3.81E-04
2	0.005	0.005636	1.66E-07	1.08E-07	2.20E-04
				Total weight	4.75E-03

Total weight of sand deposited in the 10th trial= Sand deposited at A + Sand deposited at B + Sand deposited at C

= (1.35E-02+ 7.40E-03+ 4.75E-03) kg

= 2.56E-02 kg

For Arrangement 2 of set 2 of octahedron field model layout for medium depth of flow

Table 4.59: Estimation of sediment deposition in the octahedron field at section A of Arrangement 2 of set 2 for medium depth of flow

Distance along the length of the channel (m)	Ripple Height	Radius of Cone (r)	Total Volume of sand	Volume of sand taking porosity into consideration	Weight of sand trapped (kg)
	'h' (m)	in (m)	V= (∏r² h)/3	(m^3)	W= ∂ V'
		r=h/tan Ø		V' = V-35% V	∂ = 2040 Kg/m^3
		Ø= 29°	E=10^		
0	0.026	0.0293076	2.34E-05	1.52E-05	3.10E-02
0.5	0.015	0.0169082	4.49E-06	2.92E-06	5.95E-03
1	0.011	0.0123994	1.77E-06	1.15E-06	2.35E-03
1.5	0.011	0.0123994	1.77E-06	1.15E-06	2.35E-03
2	0.006	0.0067633	2.87E-07	1.87E-07	3.81E-04
				Total weight	4.20E-02

Table 4.60: Estimation of sediment deposition in the octahedron field at section B of Arrangement 2 of set 2 for medium depth of flow

Distance along the length of the channel (m)	Ripple Height	Radius of Cone (r)	Total Volume of sand	Volume of sand taking porosity into consideration	Weight of sand trapped (kg)
	'h' (m)	in (m)	V= (∏r² h)/3	(m^3)	W= ∂ V'
		r=h/tan Ø		V' = V-35% V	∂ = 2040 Kg/m^3
		Ø= 29°	E=10^		
0	0.014	0.015781	3.65E-06	2.37E-06	4.84E-03
0.5	0.012	0.01352657	2.30E-06	1.49E-06	3.05E-03
1	0.009	0.01014493	9.70E-07	6.30E-07	1.29E-03
1.5	0.007	0.0078905	4.56E-07	2.97E-07	6.05E-04
2	0.004	0.00450886	8.51E-08	5.53E-08	1.13E-04
				Total weight	9.89E-03

Table 4.61: Estimation of sediment deposition in the octahedron field at section C of Arrangement 2 of set 2 for medium depth of flow

Distance along the length of the channel (m)	Ripple Height	Radius of Cone (r)	Total Volume of sand	Volume of sand taking porosity into consideration	Weight of sand trapped (kg)
	'h' (m)	in (m)	V= (∏r² h)/3	(m^3)	W= ∂ V'
		r=h/tan Ø		V' = V-35% V	∂ = 2040 Kg/m^3
		Ø= 29°	E=10^		
0	0.011	0.012399	1.77E-06	1.15E-06	2.35E-03
0.5	0.008	0.009018	6.81E-07	4.43E-07	9.03E-04
1	0.008	0.009018	6.81E-07	4.43E-07	9.03E-04
1.5	0.006	0.006763	2.87E-07	1.87E-07	3.81E-04
2	0.005	0.005636	1.66E-07	1.08E-07	2.20E-04
				Total weight	4.75E-03

Total weight of sand deposited in the 11th trial= Sand deposited at A + Sand deposited at B + Sand deposited at C

= (4.20E-02+ 9.89E-03+ 4.75E-03) kg

= 5.67E-02 kg

For Arrangement 2 of set 2 of octahedron field model layout for High depth of flow

Table 4.62: Estimation of sediment deposition in the octahedron field at section A of Arrangement 2 of set 2 for high depth of flow

Distance along the length of the channel (m)	Ripple Height	Radius of Cone (r)	Total Volume of sand	Volume of sand taking porosity into consideration	Weight of sand trapped (kg)
	'h' (m)	in (m)	V= (∏r² h)/3	(m³)	W= ∂ V'
		r=h/tan Ø		V' = V-35% V	∂ = 2040 Kg/m³
		Ø= 29°	E=10^		
0	0.01	0.0112721	1.33E-06	8.64E-07	1.76E-03
0.5	0.012	0.0135266	2.30E-06	1.49E-06	3.05E-03
1	0.03	0.0338164	3.59E-05	2.33E-05	4.76E-02
1.5	0.009	0.0101449	9.70E-07	6.30E-07	1.29E-03
2	0.006	0.0067633	2.87E-07	1.87E-07	3.81E-04
				Total weight	5.41E-02

Table 4.63: Estimation of sediment deposition in the octahedron field at section B of Arrangement 2 of set 2 for high depth of flow

Distance along the length of the channel (m)	Ripple Height	Radius of Cone (r)	Total Volume of sand	Volume of sand taking porosity into consideration	Weight of sand trapped (kg)
	'h' (m)	in (m)	V= (∏r² h)/3	(m^3)	W= ∂ V'
		r=h/tan Ø		V' = V-35% V	∂ = 2040 Kg/m^3
		Ø= 29°	E=10^		
0	0.009	0.01014493	9.70E-07	6.30E-07	1.29E-03
0.5	0.008	0.00901771	6.81E-07	4.43E-07	9.03E-04
1	0.005	0.00563607	1.66E-07	1.08E-07	2.20E-04
1.5	0.007	0.0078905	4.56E-07	2.97E-07	6.05E-04
2	0.004	0.00450886	8.51E-08	5.53E-08	1.13E-04
				Total weight	3.13E-03

Table 4.64: Estimation of sediment deposition in the octahedron field at section C of Arrangement 2 of set 2 for high depth of flow

Distance along the length of the channel (m)	Ripple Height	Radius of Cone (r)	Total Volume of sand	Volume of sand taking porosity into consideration	Weight of sand trapped (kg)
	'h' (m)	in (m)	V= (∏r² h)/3	(m^3)	W= ∂ V'
		r=h/tan Ø		V' = V-35% V	∂ = 2040 Kg/m^3
		Ø= 29°	E=10^		
0	0.002	0.002254	1.06E-08	6.92E-09	1.41E-05
0.5	0.01	0.011272	1.33E-06	8.64E-07	1.76E-03
1	0.003	0.003382	3.59E-08	2.33E-08	4.76E-05
1.5	0.001	0.001127	1.33E-09	8.64E-10	1.76E-06
2	0.001	0.001127	1.33E-09	8.64E-10	1.76E-06
				Total weight	1.83E-03

Total weight of sand deposited in the 12th trial= Sand deposited at A + Sand deposited at B + Sand deposited at C

= (5.41E-02+ 3.13E-03+ 1.83E-03) kg

= 5.90E-02 kg

For Arrangement 1 of set 3 of octahedron field model layout for low depth of flow

Table 4.65: Estimation of sediment deposition in the octahedron field at section A of Arrangement 1 of set 3 for low depth of flow

Distance along the length of the channel (m)	Ripple Height	Radius of Cone (r)	Total Volume of sand	Volume of sand taking porosity into consideration	Weight of sand trapped (kg)
	'h' (m)	in (m)	V= (∏r² h)/3	(m^3)	W= ∂ V'
		r=h/tan Ø		V' = V-35% V	∂ = 2040 Kg/m^3
		Ø= 29°	E=10^		
0	0.016	0.018035	5.45E-06	3.54E-06	7.22E-03
0.5	0.017	0.019163	6.53E-06	4.25E-06	8.66E-03
1	0.0011	0.00124	1.77E-09	1.15E-09	2.35E-06
1.5	0.008	0.009018	6.81E-07	4.43E-07	9.03E-04
2	0.006	0.006763	2.87E-07	1.87E-07	3.81E-04
				total weight	1.72E-02

Table 4.66: Estimation of sediment deposition in the octahedron field at section B of Arrangement 1 of set 3 for low depth of flow

Distance along the length of the channel (m)	Ripple Height	Radius of Cone (r)	Total Volume of sand	Volume of sand taking porosity into consideration	Weight of sand trapped (kg)
	'h' (m)	in (m)	V= (∏r² h)/3	(m^3)	W= ∂ V'
		r=h/tan Ø		V' = V-35% V	∂ = 2040 Kg/m^3
		Ø= 29°	E=10^		
0	0.009	0.01014493	9.70E-07	6.30E-07	1.29E-03
0.5	0.01	0.01127214	1.33E-06	8.64E-07	1.76E-03
1	0.007	0.0078905	4.56E-07	2.97E-07	6.05E-04
1.5	0.006	0.00676329	2.87E-07	1.87E-07	3.81E-04
2	0.004	0.00450886	8.51E-08	5.53E-08	1.13E-04
				total weight	4.15E-03

Table 4.67: Estimation of sediment deposition in the octahedron field at section C of Arrangement 1 of set 3 for low depth of flow

Distance along the length of the channel (m)	Ripple Height	Radius of Cone (r)	Total Volume of sand	Volume of sand taking porosity into consideration	Weight of sand trapped (kg)
	'h' (m)	in (m)	V= (∏r² h)/3	(m^3)	W= ∂ V'
		r=h/tan Ø		V' = V-35% V	∂ = 2040 Kg/m^3
		Ø= 29°	E=10^		
0	0.009	0.010145	9.70E-07	6.30E-07	1.29E-03
0.5	0.008	0.009018	6.81E-07	4.43E-07	9.03E-04
1	0.008	0.009018	6.81E-07	4.43E-07	9.03E-04
1.5	0.006	0.006763	2.87E-07	1.87E-07	3.81E-04
2	0.005	0.005636	1.66E-07	1.08E-07	2.20E-04
				total weight	3.69E-03

Total weight of sand deposited in the 13th trial= Sand deposited at A + Sand deposited at B + Sand deposited at C

= (1.72E-02+ 4.15E-03+3.69E-03) kg

= 2.50E-02 kg

For Arrangement 1 of set 3 of octahedron field model layout for medium depth of flow

Table 4.68: Estimation of sediment deposition in the octahedron field at section A of Arrangement 1 of set 3 for medium depth of flow

Distance along the length of the channel (m)	Ripple Height	Radius of Cone (r)	Total Volume of sand	Volume of sand taking porosity into consideration	Weight of sand trapped (kg)
	'h' (m)	in (m)	V= (∏r² h)/3	(m^3)	W= ∂ V'
		r=h/tan Ø		V' = V-35% V	∂ = 2040 Kg/m^3
		Ø= 29°	E=10^		
0	0.009	0.010145	9.70E-07	6.30E-07	1.29E-03
0.5	0.008	0.009018	6.81E-07	4.43E-07	9.03E-04
1	0.007	0.00789	4.56E-07	2.97E-07	6.05E-04
1.5	0.006	0.006763	2.87E-07	1.87E-07	3.81E-04
2	0.005	0.005636	1.66E-07	1.08E-07	2.20E-04
				total weight	3.39E-03

Table 4.69: Estimation of sediment deposition in the octahedron field at section B of Arrangement 1 of set 3 for medium depth of flow

Distance along the length of the channel (m)	Ripple Height	Radius of Cone (r)	Total Volume of sand	Volume of sand taking porosity into consideration	Weight of sand trapped (kg)
	'h' (m)	in (m)	V= (∏r² h)/3	(m^3)	W= ∂ V'
		r=h/tan Ø		V' = V-35% V	∂ = 2040 Kg/m^3
		Ø= 29°	E=10^		
0	0.013	0.01465378	2.92E-06	1.90E-06	3.87E-03
0.5	0.012	0.01352657	2.30E-06	1.49E-06	3.05E-03
1	0.009	0.01014493	9.70E-07	6.30E-07	1.29E-03
1.5	0.007	0.0078905	4.56E-07	2.97E-07	6.05E-04
2	0.004	0.00450886	8.51E-08	5.53E-08	1.13E-04
				total weight	8.92E-03

Table 4.70: Estimation of sediment deposition in the octahedron field at section C of Arrangement 1 of set 3 for medium depth of flow

Distance along the length of the channel (m)	Ripple Height	Radius of Cone (r)	Total Volume of sand	Volume of sand taking porosity into consideration	Weight of sand trapped (kg)
	'h' (m)	in (m)	V= (∏r² h)/3	(m^3)	W= ∂ V'
		r=h/tan Ø		V' = V-35% V	∂ = 2040 Kg/m^3
		Ø= 29°	E=10^		
0	0.02	0.022544	1.06E-05	6.92E-06	1.41E-02
0.5	0.015	0.016908	4.49E-06	2.92E-06	5.95E-03
1	0.017	0.019163	6.53E-06	4.25E-06	8.66E-03
1.5	0.011	0.012399	1.77E-06	1.15E-06	2.35E-03
2	0.006	0.006763	2.87E-07	1.87E-07	3.81E-04
				total weight	3.15E-02

Total weight of sand deposited in the 14th trial= Sand deposited at A + Sand deposited at B + Sand deposited at C

= (3.39E-03+ 8.92E-03+3.15E-02) kg

= 4.38E-02 kg

For Arrangement 1 of set 3 of octahedron field model layout for High depth of flow

Table 4.71: Estimation of sediment deposition in the octahedron field at section A of Arrangement 1 of set 3 for high depth of flow

Distance along the length of the channel (m)	Ripple Height	Radius of Cone (r)	Total Volume of sand	Volume of sand taking porosity into consideration	Weight of sand trapped (kg)
	'h' (m)	in (m)	V= (∏r² h)/3	(m^3)	W= ∂ V'
		r=h/tan Ø		V' = V-35% V	∂ = 2040 Kg/m^3
		Ø= 29°	E=10^		
0	0.01	0.011272	1.33E-06	8.64E-07	1.76E-03
0.5	0.009	0.010145	9.70E-07	6.30E-07	1.29E-03
1	0.007	0.00789	4.56E-07	2.97E-07	6.05E-04
1.5	0.006	0.006763	2.87E-07	1.87E-07	3.81E-04
2	0.002	0.002254	1.06E-08	6.92E-09	1.41E-05
				total weight	4.05E-03

Table 4.72: Estimation of sediment deposition in the octahedron field at section B of Arrangement 1 of set 3 for high depth of flow

Distance along the length of the channel (m)	Ripple Height	Radius of Cone (r)	Total Volume of sand	Volume of sand taking porosity into consideration	Weight of sand trapped (kg)
	'h' (m)	in (m)	V= (∏r² h)/3	(m³)	W= ∂ V'
		r=h/tan Ø		V' = V-35% V	∂ = 2040 Kg/m³
		Ø= 29°	E=10^		
0	0.011	0.01239936	1.77E-06	1.15E-06	2.35E-03
0.5	0.012	0.01352657	2.30E-06	1.49E-06	3.05E-03
1	0.009	0.01014493	9.70E-07	6.30E-07	1.29E-03
1.5	0.007	0.0078905	4.56E-07	2.97E-07	6.05E-04
2	0.004	0.00450886	8.51E-08	5.53E-08	1.13E-04
				total weight	7.40E-03

Table 4.73: Estimation of sediment deposition in the octahedron field at section C of Arrangement 1 of set 3 for high depth of flow

Distance along the length of the channel (m)	Ripple Height	Radius of Cone (r)	Total Volume of sand	Volume of sand taking porosity into consideration	Weight of sand trapped (kg)
	'h' (m)	in (m)	V= (∏r² h)/3	(m^3)	W= ∂ V'
		r=h/tan Ø		V' = V-35% V	∂ = 2040 Kg/m^3
		Ø= 29°	E=10^		
0	0.017	0.019163	6.53E-06	4.25E-06	8.66E-03
0.5	0.02	0.022544	1.06E-05	6.92E-06	1.41E-02
1	0.02	0.022544	1.06E-05	6.92E-06	1.41E-02
1.5	0.011	0.012399	1.77E-06	1.15E-06	2.35E-03
2	0.006	0.006763	2.87E-07	1.87E-07	3.81E-04
				total weight	3.96E-02

Total weight of sand deposited in the 15th trial= Sand deposited at A + Sand deposited at B + Sand deposited at C

= (4.05E-03+ 7.40E-03+ 3.96E-02) kg

= 5.11E-02 kg

For Arrangement 2 of set 3 of octahedron field model layout for low depth of flow

Table 4.74: Estimation of sediment deposition in the octahedron field at section A of Arrangement 2 of set 3 for low depth of flow

Distance along the length of the channel (m)	Ripple Height	Radius of Cone (r)	Total Volume of sand	Volume of sand taking porosity into consideration	Weight of sand trapped (kg)
	'h' (m)	in (m)	V= (∏r² h)/3	(m³)	W= ∂ V'
		r=h/tan Ø		V' = V-35% V	∂ = 2040 Kg/m³
		Ø= 29°	E=10^		
0	0.013	0.014654	2.92E-06	1.90E-06	3.87E-03
0.5	0.015	0.016908	4.49E-06	2.92E-06	5.95E-03
1	0.0011	0.00124	1.77E-09	1.15E-09	2.35E-06
1.5	0.008	0.009018	6.81E-07	4.43E-07	9.03E-04
2	0.006	0.006763	2.87E-07	1.87E-07	3.81E-04
				total weight	1.11E-02

Table 4.75: Estimation of sediment deposition in the octahedron field at section B of Arrangement 2 of set 3 for low depth of flow

Distance along the length of the channel (m)	Ripple Height	Radius of Cone (r)	Total Volume of sand	Volume of sand taking porosity into consideration	Weight of sand trapped (kg)
	'h' (m)	in (m)	V= (∏r² h)/3	(m^3)	W= ∂ V'
		r=h/tan Ø		V' = V-35% V	∂ = 2040 Kg/m^3
		Ø= 29°	E=10^		
0	0.011	0.01239936	1.77E-06	1.15E-06	2.35E-03
0.5	0.012	0.01352657	2.30E-06	1.49E-06	3.05E-03
1	0.009	0.01014493	9.70E-07	6.30E-07	1.29E-03
1.5	0.007	0.0078905	4.56E-07	2.97E-07	6.05E-04
2	0.004	0.00450886	8.51E-08	5.53E-08	1.13E-04
				total weight	7.40E-03

Table 4.76: Estimation of sediment deposition in the octahedron field at section C of Arrangement 2 of set 3 for low depth of flow

Distance along the length of the channel (m)	Ripple Height	Radius of Cone (r)	Total Volume of sand	Volume of sand taking porosity into consideration	Weight of sand trapped (kg)
	'h' (m)	in (m)	V= (∏r² h)/3	(m^3)	W= ∂ V'
		r=h/tan Ø		V' = V-35% V	∂ = 2040 Kg/m^3
		Ø= 29°	E=10^		
0	0.009	0.010145	9.70E-07	6.30E-07	1.29E-03
0.5	0.008	0.009018	6.81E-07	4.43E-07	9.03E-04
1	0.008	0.009018	6.81E-07	4.43E-07	9.03E-04
1.5	0.006	0.006763	2.87E-07	1.87E-07	3.81E-04
2	0.005	0.005636	1.66E-07	1.08E-07	2.20E-04
				total weight	3.69E-03

Total weight of sand deposited in the 16th trial= Sand deposited at A + Sand deposited at B + Sand deposited at C

= (1.11E-02+ 7.40E-03+3.69E-03) kg

= 2.22E-02 kg

For Arrangement 2 of set 3 of octahedron field model layout for medium depth of flow

Table 4.77: Estimation of sediment deposition in the octahedron field at section A of Arrangement 2 of set 3 for medium depth of flow

Distance along the length of the channel (m)	Ripple Height	Radius of Cone (r)	Total Volume of sand	Volume of sand taking porosity into consideration	Weight of sand trapped (kg)
	'h' (m)	in (m)	V= (∏r² h)/3	(m³)	W= ∂ V'
		r=h/tan Ø		V' = V-35% V	∂ = 2040 Kg/m³
		Ø= 29°	E=10^		
0	0.02	0.022544	1.06E-05	6.92E-06	1.41E-02
0.5	0.018	0.02029	7.76E-06	5.04E-06	1.03E-02
1	0.0021	0.002367	1.23E-08	8.01E-09	1.63E-05
1.5	0.011	0.012399	1.77E-06	1.15E-06	2.35E-03
2	0.006	0.006763	2.87E-07	1.87E-07	3.81E-04
				total weight	2.71E-02

Table 4.78: Estimation of sediment deposition in the octahedron field at section B of Arrangement 2 of set 3 for medium depth of flow

Distance along the length of the channel (m)	Ripple Height	Radius of Cone (r)	Total Volume of sand	Volume of sand taking porosity into consideration	Weight of sand trapped (kg)
	'h' (m)	in (m)	V= (∏r² h)/3	(m^3)	W= ∂ V'
		r=h/tan Ø		V' = V-35% V	∂ = 2040 Kg/m^3
		Ø= 29°	E=10^		
0	0.014	0.015781	3.65E-06	2.37E-06	4.84E-03
0.5	0.012	0.01352657	2.30E-06	1.49E-06	3.05E-03
1	0.009	0.01014493	9.70E-07	6.30E-07	1.29E-03
1.5	0.007	0.0078905	4.56E-07	2.97E-07	6.05E-04
2	0.004	0.00450886	8.51E-08	5.53E-08	1.13E-04
				total weight	9.89E-03

Table 4.79: Estimation of sediment deposition in the octahedron field at section C of Arrangement 2 of set 3 for medium depth of flow

Distance along the length of the channel (m)	Ripple Height	Radius of Cone (r)	Total Volume of sand	Volume of sand taking porosity into consideration	Weight of sand trapped (kg)
	'h' (m)	in (m)	V= (∏r² h)/3	(m^3)	W= ∂ V'
		r=h/tan Ø		V' = V-35% V	∂ = 2040 Kg/m^3
		Ø= 29°	E=10^		
0	0.009	0.010145	9.70E-07	6.30E-07	1.29E-03
0.5	0.008	0.009018	6.81E-07	4.43E-07	9.03E-04
1	0.008	0.009018	6.81E-07	4.43E-07	9.03E-04
1.5	0.006	0.006763	2.87E-07	1.87E-07	3.81E-04
2	0.005	0.005636	1.66E-07	1.08E-07	2.20E-04
				total weight	3.69E-03

Total weight of sand deposited in the 17th trial= Sand deposited at A + Sand deposited at B + Sand deposited at C

= (2.71E-02+ 9.89E-03+3.69E-03) kg

= 4.07E-02 kg

For Arrangement 2 of set 3 of octahedron field model layout for High depth of flow

Table 4.80 Estimation of sediment deposition in the octahedron field at section A of Arrangement 2 of set 3 for high depth of flow

Distance along the length of the channel (m)	Ripple Height	Radius of Cone (r)	Total Volume of sand	Volume of sand taking porosity into consideration	Weight of sand trapped (kg)
	'h' (m)	in (m)	V= (∏r² h)/3	(m³)	W= ∂ V'
		r=h/tan Ø		V' = V-35% V	∂ = 2040 Kg/m³
		Ø= 29°	E=10^		
0	0.02	0.022544	1.06E-05	6.92E-06	1.41E-02
0.5	0.017	0.019163	6.53E-06	4.25E-06	8.66E-03
1	0.02	0.022544	1.06E-05	6.92E-06	1.41E-02
1.5	0.011	0.012399	1.77E-06	1.15E-06	2.35E-03
2	0.006	0.006763	2.87E-07	1.87E-07	3.81E-04
				total weight	3.96E-02

Table 4.81 Estimation of sediment deposition in the octahedron field at section B of Arrangement 2 of set 3 for high depth of flow

Distance along the length of the channel (m)	Ripple Height	Radius of Cone (r)	Total Volume of sand	Volume of sand taking porosity into consideration	Weight of sand trapped (kg)
	'h' (m)	in (m)	V= (∏r² h)/3	(m³)	W= ∂ V'
		r=h/tan Ø		V' = V-35% V	∂ = 2040 Kg/m³
		Ø= 29°	E=10^		
0	0.01	0.01127214	1.33E-06	8.64E-07	1.76E-03
0.5	0.012	0.01352657	2.30E-06	1.49E-06	3.05E-03
1	0.009	0.01014493	9.70E-07	6.30E-07	1.29E-03
1.5	0.007	0.0078905	4.56E-07	2.97E-07	6.05E-04
2	0.004	0.00450886	8.51E-08	5.53E-08	1.13E-04
				total weight	6.81E-03

Table 4.82: Estimation of sediment deposition in the octahedron field at section C of Arrangement 2 of set 3 for high depth of flow

Distance along the length of the channel (m)	Ripple Height	Radius of Cone (r)	Total Volume of sand	Volume of sand taking porosity into consideration	Weight of sand trapped (kg)
	'h' (m)	in (m)	V= (∏r² h)/3	(m^3)	W= ∂ V'
		r=h/tan Ø		V' = V-35% V	∂ = 2040 Kg/m^3
		Ø= 29°	E=10^		
0	0.009	0.010145	9.70E-07	6.30E-07	1.29E-03
0.5	0.01	0.011272	1.33E-06	8.64E-07	1.76E-03
1	0.008	0.009018	6.81E-07	4.43E-07	9.03E-04
1.5	0.005	0.005636	1.66E-07	1.08E-07	2.20E-04
2	0.003	0.003382	3.59E-08	2.33E-08	4.76E-05
				total weight	4.22E-03

Total weight of sand deposited in the 18th trial= Sand deposited at A + Sand deposited at B + Sand deposited at C

= (3.96E-02+ 6.81E-03+ 4.22E-03) kg

= 5.06E-02 kg

CHAPTER 5

RESULT AND DISCUSSION

In this chapter the analysis of the experiments are presented the data recorded and calculated as in chapter 4 of this report has been analysed in this chapter for finding conclusions of the experimental work

5.1 CALCULATION OF TRAP EFFICIENCY

Trap efficiency has been calculated for the different orientation of the Octahedron fields and varying depth of flow.

Table 5.1: Trap Efficiency for Arrangement 1

Set No.	Inclination of diversion line to retard (in degrees)	SDR	Depth of flow	Weight of sand deposited	weight of sand injected	trap Efficiency (%)
1	90	0.958	Low	0.02081584	3	0.693861
	90	0.7	Medium	0.03281264	3	1.093755
	90	0.5	High	0.04837867	3	1.612622
2	60	0.965	Low	0.03166992	3	1.055664
	60	0.7	Medium	0.0563429	3	1.878097
	60	0.5	High	0.06184972	3	2.061657
3	45	0.965	Low	0.02501345	3	0.833782
	45	0.7	Medium	0.04377076	3	1.459025
	45	0.5	High	0.05105384	3	1.701795

Table 5.2: Trap Efficiency for Arrangement 2

Set No.	Inclination of diversion line to retard (in degrees)	SDR	Depth of flow	Weight of sand deposited	weight of sand injected	trap Efficiency (%)
1	90	1.076	Low	0.01964491	3	0.65483
	90	0.7777	Medium	0.03098746	3	1.032915
	90	0.538	High	0.04410053	3	1.470018
2	90	1.076	Low	0.02560892	3	0.853631
	90	0.7777	Medium	0.05666516	3	1.888839
	90	0.538	High	0.05904582	3	1.968194
3	90	1.076	Low	0.0222025	3	0.740083
	90	0.7777	Medium	0.04071868	3	1.357289
	90	0.538	High	0.05064119	3	1.68804

5.2 ANALYSIS OF VELOCITY REDUCTION DUE TO OCTAHEDRONS

Velocity was measured using Acoustic Doppler velocimeter (ADV) for all the 3 experimental set up for different depth of flow and also without the Octahedron fields. The Average velocity was calculated using the measured velocity and percentage of reduction was calculated bellow

Table 5.3 Reduction in average velocity due to presence of Octahedron field

Set No.	Depth of flow	Average velocity without Octahedron(m/s)	Average velocity with Octahedron (m/s)	Reduction (%)
1	Low	0.0941	0.0779	17.216
	Medium	0.1257	0.0979	22.116
	High	0.1305	0.0959	26.513
2	Low	0.0951	0.0655	31.125
	Medium	0.1268	0.0777	38.722
	High	0.1311	0.0751	42.715
3	Low	0.0911	0.067	26.454
	Medium	0.1243	0.0853	31.376
	High	0.1348	0.0879	34.792

Result: From the table it can be seen that velocity reduction is maximum in set no 2 where inclination angle of diversion line with retard is 60 degrees. With in the same set velocity reduction increases with increase in depth of flow. Thus octahedron are more efficient in reducing velocity when placed at 60 degree angle of inclinations of diversion line with the retard.

5.3 COMPARISON OF TRAP EFFICIENCY WITH DIFFERENT INDICES AND THEIR GRAPHICAL REPRESENTATION

The variation of trap efficiency with different factor such as submergence depth ratio, inclination of octahedron field to the retard and velocity of flow has been analysed graphically in this section.

5.3.1 Variation of trap efficiency with degree of inclination of diversion line with retard

The trap efficiency vs degree of inclination graphs has been drawn bellow and compared for the different flow depth for arrangement 1 of all the 3 sets of experiment. Degree of inclination refers to the angle between the line of diversion of the octahedron and the retard.

Table 5.4: Data for graph of trap efficiency vs angle of diversion line and retard for arrangement 1

Low Depth		Medium Depth		High Depth	
Trap efficiency	Inclination	Trap efficiency	Inclination	Trap efficiency	Inclination
0.693861445	90	1.093754652	90	1.612622406	90
1.055663986	60	1.87809677	60	2.061657274	60
0.833781803	45	1.459025324	45	1.701794535	45

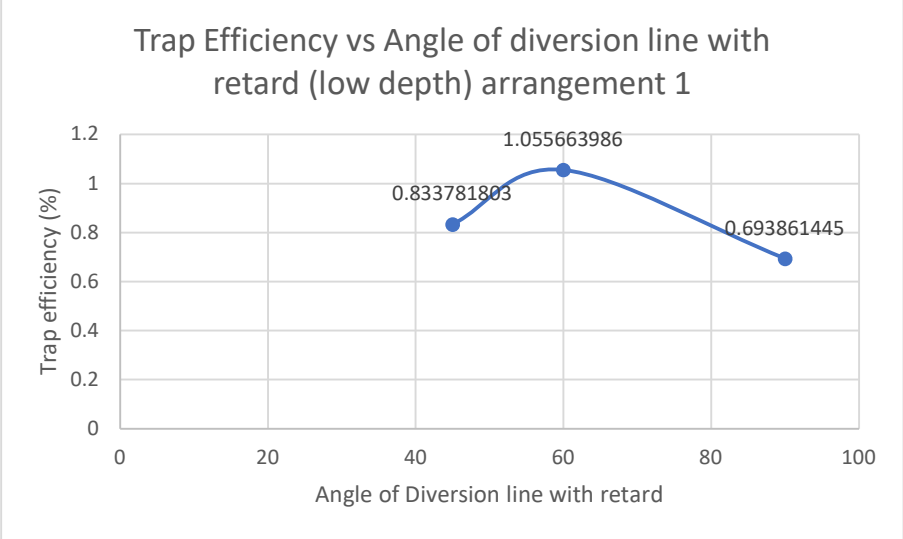

Figure. 5.1: Plot for trap efficiency vs angle of inclination of diversion line with retard for low depth of flow (Arrangement 1)

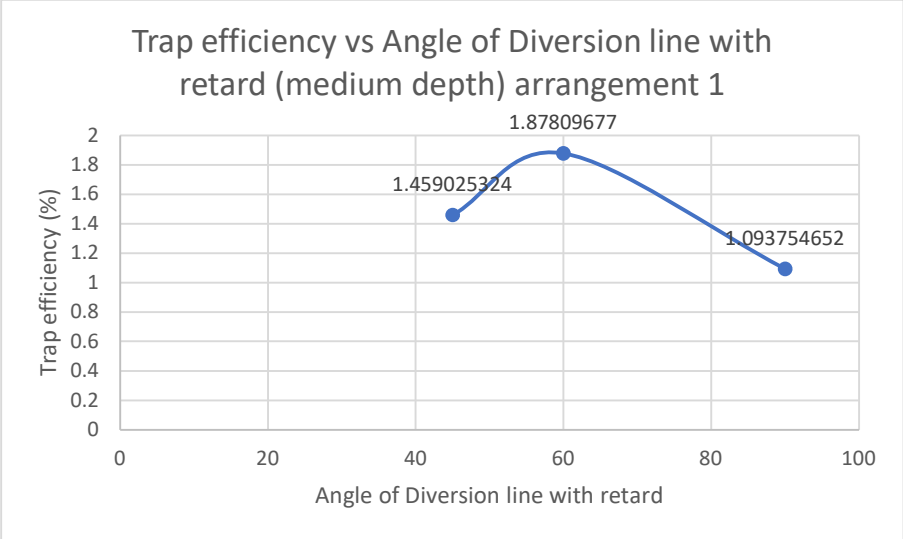

Figure. 5.2: Plot for trap efficiency vs angle of inclination of diversion line with retard for medium depth of flow (Arrangement 1)

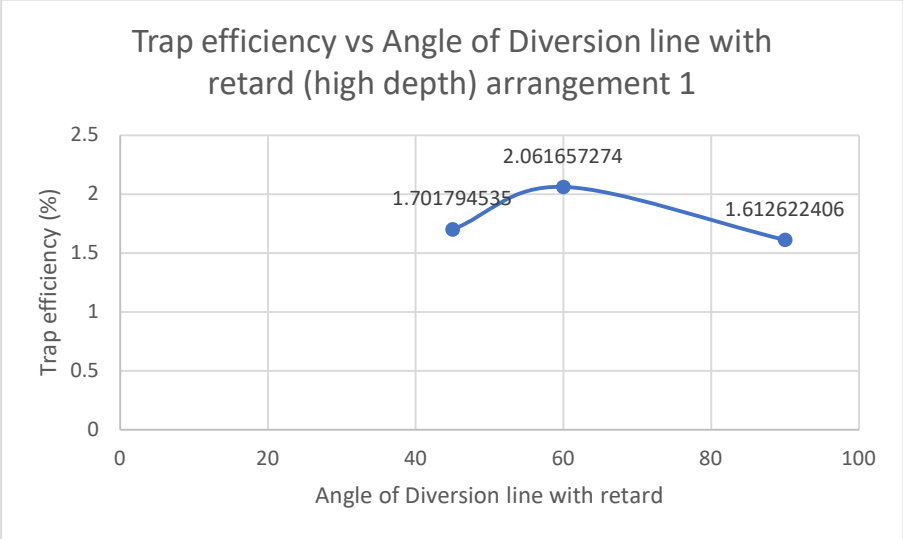

Figure. 5.3: Plot for trap efficiency vs angle of inclination of diversion line with retard for high depth of flow (Arrangement 1)

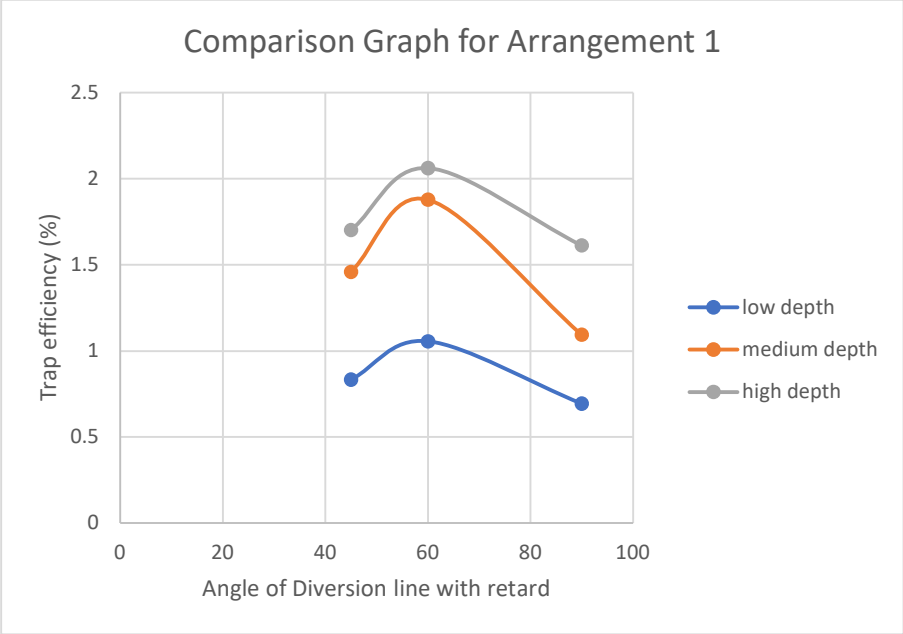

Figure 5.4: Graph for comparison of trap efficiency vs Angle between Diversion line and retard for varying depth of flow(Arrangement 1)

Result: In arrangement 1, when the angle of inclination of Diversion line of the Octahedron fields to the retard was varied as 45, 60 and 90 degrees, for different depth of flow such as low, medium and high depth of flow it is observed that trap efficiency increases with decrease in angle of inclination of diversion line with retard and it is maximum at 60-degree angle of inclination and with further decrease in angle of inclination trap efficiency started to decrease. Thus, it can be concluded that Octahedron placed at 60-degree angle of inclination of diversion line with retard will be most effective in trapping sediment in the river.

5.3.2 Variation in Arrangement 2 due to changes in Arrangement 1

As the degree of inclination of the diversion line to the retard for arrangement 1 was varied it had impact on arrangement 2. The variation in trap efficiency in arrangement 2 due to changes in arrangement 1 are analysed bellow

Table 5.5 Data for trap efficiency vs Inclination of diversion line with retard of arrangement 2 W.R.T arrangement 1

Inclination of Arrangement 1	Low Depth		Medium Depth		High Depth	
	Trap efficiency	Inclination	Trap efficiency	Inclination	Trap efficiency	Inclination
90	0.6548302	90	1.0329153	90	1.47001753	90
60	0.8536306	90	1.8888385	90	1.96819406	90
45	0.7400834	90	1.3572892	90	1.68803957	90

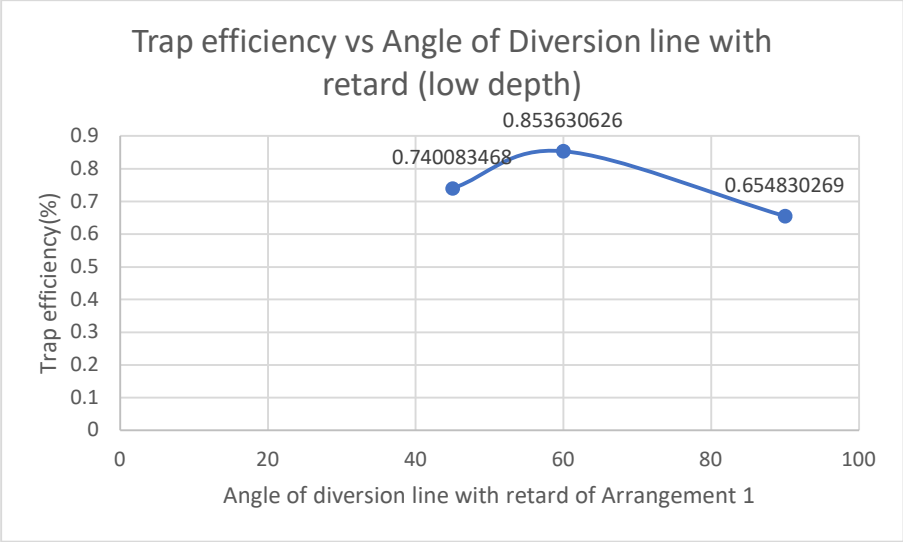

Figure. 5.5: Plot for trap efficiency vs angle of inclination of diversion line with retard for low depth of flow for Arrangement 2 w.r.t. arrangement 1

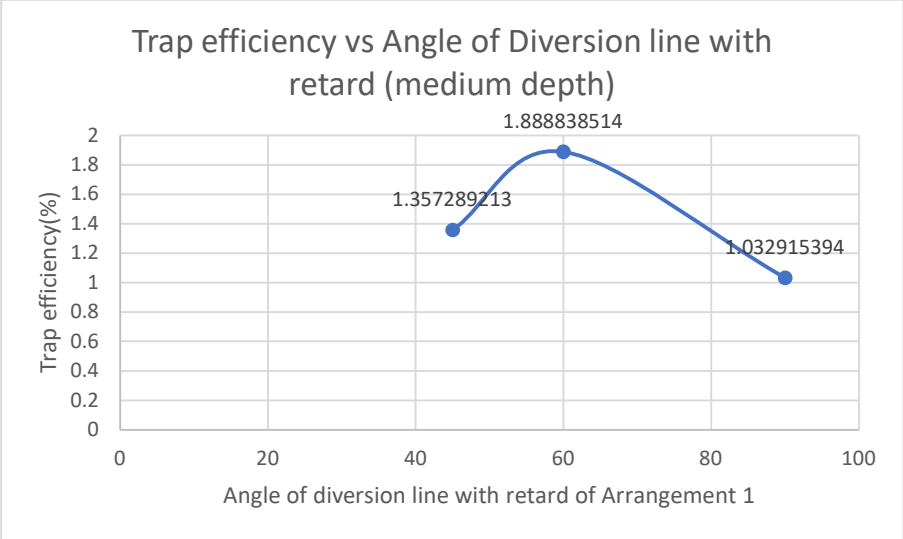

Figure. 5.6: Plot for trap efficiency vs angle of inclination of diversion line with retard for medium depth of flow for Arrangement 2 w.r.t. arrangement 1

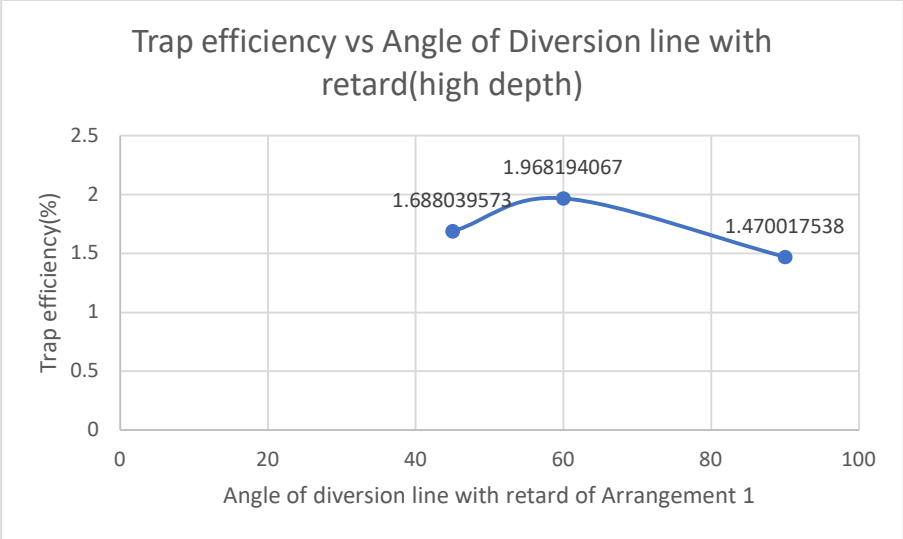

Figure. 5.7: Plot for trap efficiency vs angle of inclination of diversion line with retard for high depth of flow for Arrangement 2 w.r.t. arrangement 1

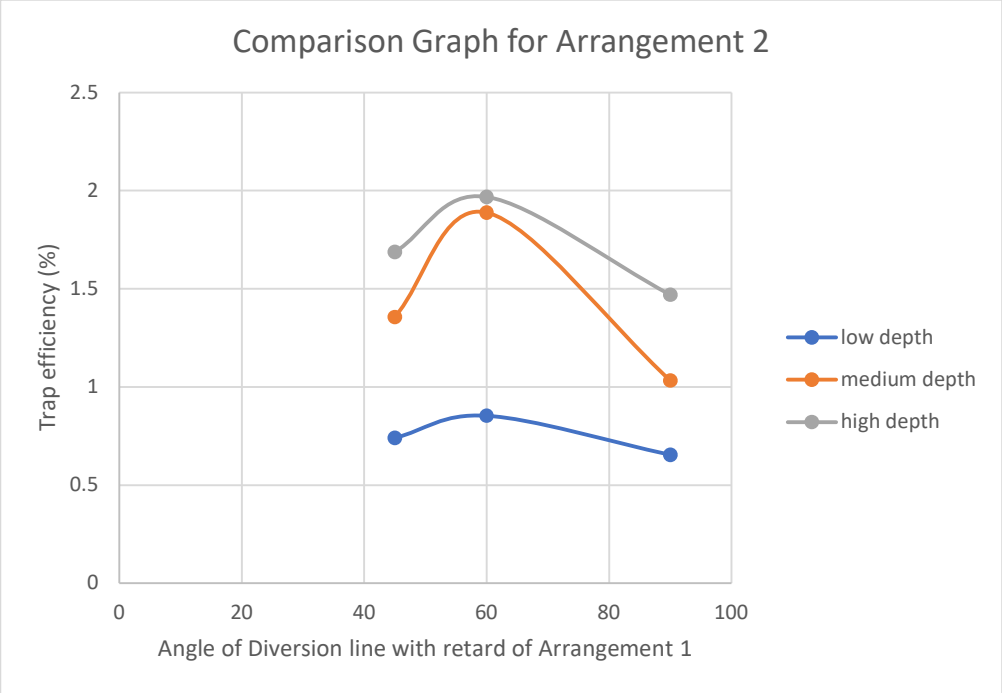

Figure. 5.8: Comparison Graph for trap efficiency vs angle of inclination of diversion line with retard for varying depth of flow for Arrangement 2 w.r.t. arrangement 1

Result: In arrangement 2 inclination of diversion line with retard was kept 90 degrees for all 3 set up to see the effects on it due to the change in inclination of arrangement 1 from 90 degree to 45 degree which was laid upstream of the arrangement 2. It can be seen that as the angle of inclination of diversion line with retard decreases in the arrangement 1 sedimentation increases in the arrangement 2. It shows similar result as arrangement 1 just trap efficiency is less in arrangement 2 than arrangement 1. Comparing the all three depth of flow, trap efficiency at arrangement 2 with respect to 60-degree inclination of arrangement 1 at high depth of flow was found to be highest.

5.3.3 Variation of trap efficiency with Submergence depth ratio

Variation of trap efficiency with submergence depth ratio has been shown by drawing graph for different flow depth, for both the arrangements (1 and 2)

Table 5.6 Data for SDR vs trap efficiency graph for Arrangement 1

Submergence depth ratio (SDR)	Trap efficiency (%) for inclination of diversion line with retard		
	90 degrees	60 degrees	45 degrees
0.958	0.693861445	1.055663986	0.83378
0.7	1.093754652	1.87809677	1.45903
0.5	1.612622406	2.061657274	1.70179

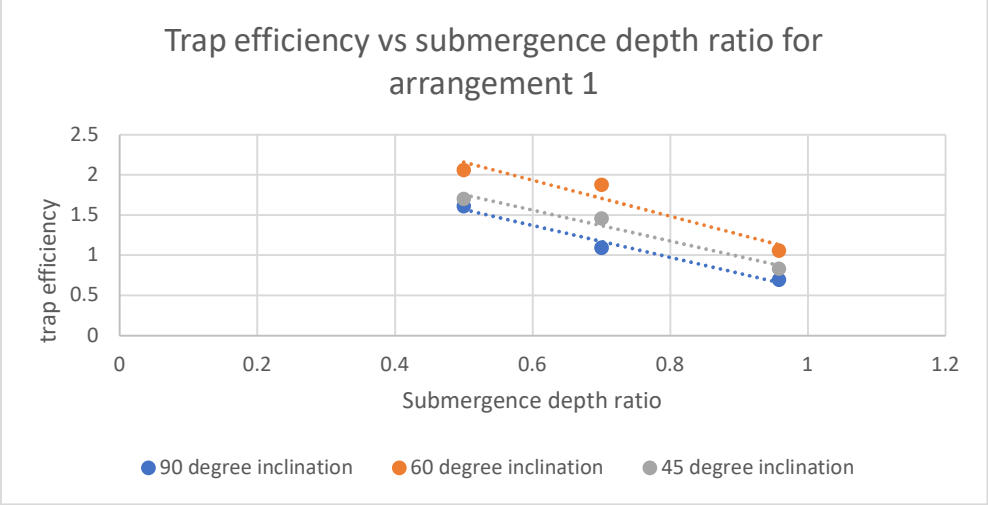

Figure 5.9 plot for trap efficiency vs SDR for arrangement 1

Here inclination means angle of diversion line with retard

Result: From the graph 5.9 it can be concluded that in arrangement 1 with the increase in SDR trap efficiency deceases for different angle of inclination of diversion line with retard. High SDR indicate low depth of flow and low SDR indicate high depth of flow. So we can conclude trap efficiency is directly proportional to depth of flow or trap efficiency is indirectly proportional to SDR

Table 5.7 Data for SDR vs trap efficiency graph for Arrangement 2

Submergence depth ratio	Trap efficiency (%) for inclination of diversion line with retard		
	90 degrees	60 degrees	45 degrees
1.07	0.65483027	0.8536306	0.74008347
0.7777	1.03291539	1.8888385	1.35728921
0.538	1.47001754	1.9681941	1.68803957

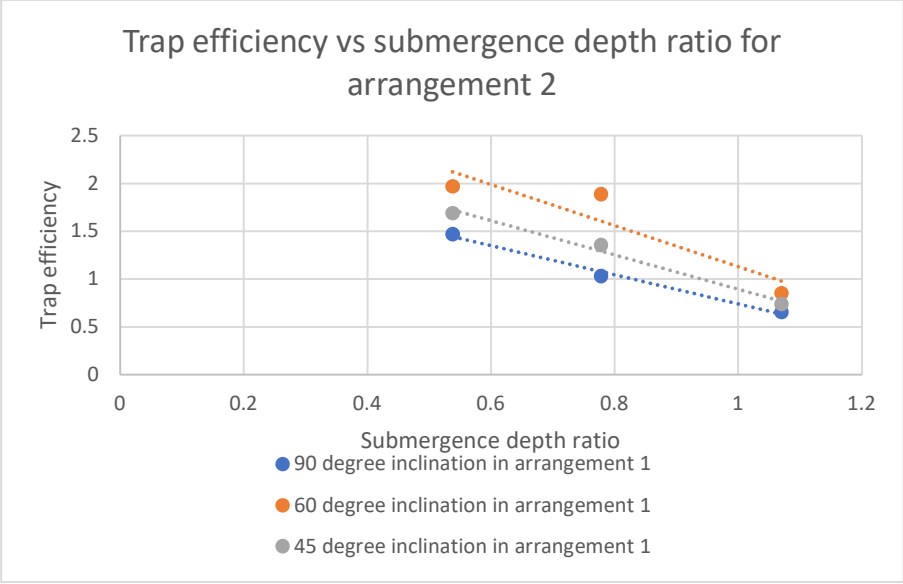

Figure 5.10 plot for trap efficiency vs SDR for arrangement 2

Result: From the graph 5.10 it can be concluded that in arrangement 2 with the increase in SDR trap efficiency deceases for different angle of inclination of diversion line with retard in the arrangement 1. High SDR indicate low depth of flow and low SDR indicate high depth of flow. So we can conclude trap efficiency is directly proportional to depth of flow or trap efficiency is indirectly proportional to SDR

CHAPTER 6

CONCLUSION

6.1 SUMMARY

In this project existing Jack Jetty structure is modified in to a new model called “Octahedron”, with the intension of better stability and increasing sediment trap efficiency. The experiment is done in 3 different type of set up, each setup having two arrangement. Setups were made based on angle of inclination of diversion line of the octahedron field to the retard of the octahedron field. The depth of flow of water was varied from low, medium to high for each set up and sediment deposition was measured in gridded pattern in both the arrangements. Using sediment deposition data trap efficiency were calculated and analysed with respect to other factors such as submergence depth ratio (SDR), degree of inclination of diversion line with retard. The contour plots were then drawn for better representation of sediment deposition. Using Acoustic Doppler Velocimeter (ADV) velocity of flow were measured. Effect on velocity due to Octahedron field were also compared.

The following conclusions can be drawn from all the experiments and analysis that have been performed in the study-

1. Trap efficiency increases with increase in angle of inclination of divergent line of octahedron field with retard of octahedron field become maximum at 30-degree angle of inclination of divergent line with flow direction and then started decrease.
2. Due to presence of the octahedron field at the outer bank, scouring effect was reduced dramatically and bank was protected.
3. Trap efficiency depend on Submergence depth ratio (SDR) which is a function of depth of flow. Thus, it can be concluded that trap efficiency is also a function of depth of flow.
4. With increase in depth of flow SDR decreases and trap efficiency increases. Thus, trap efficiency is inversely proportional to SDR.
5. Due to the presence of octahedron field velocity of water decreases. Reduction in velocity is maximum at 60 degrees angle of inclination of diversion line with retard.

The application of octahedron system is an effective and economic method for river training purpose. It serves the purpose of prevention of scouring by deposition of sediments facilitated by the significant decrease in intensity of flow caused by a decrease in the velocity of flow by the octahedron. The fabrication of these structures is simple, requiring only concrete and steel rods, with a few numbers of nuts and bolts only. Due to their symmetrical structure Their installation can be done by just placing them successively and connecting them together using wire rope, thus needing no skilful labour.

6.2 FUTURE SCOPE

There has been some limitations and drawbacks while performing the experiments, which can be overcome in future studies

1. To find out the sediment deposition pattern more orientation and arrangement of octahedron field can be studied for more reliable value.
2. Octahedron are not tested in real field yet. Which can be done in future to see its practical expects.
3. In this study same amount of sediment and same type of sediments were used for all the experiments. Further study can be done by varying the size and quantity of sediment.
4. Comparative study of different models such as porcupine, jack jetty or other permeable structure can be done.

REFERENCES

1. Aamir M. and Sharma N. (2014), "Sediment Trap Efficiency of Porcupine Systems for Riverbank Protection". ISH-HYDRO 2014 INTERNATIONAL.
2. Aamir M. and Sharma N. (2015), "Efficiency of Triangular and Prismatic Porcupines in Capturing Sediment for River raining". HYDRO 2015 INTERNATIONAL. 20th International Conference on hydraulics, Water Resources and River Engineering.
3. Abhigya Shriwastava, and Nayan Sharmar (2014), "Investigation of RCC Jack Jetty as a Cost-Effective River Training Structure", T International Conference on Agricultural, Environmental and Biological Sciences (AEBS-2014) Phuket (Thailand)
4. Foley, M.G. (1979), "Mechanics of sediment transportation and alluvial stream problems", R. J. Garde and K. G. Ranga Raju, Halsted Press, New York (Wiley Eastern Limited, New Delhi), 1977. No. of pages: 483. Earth Surf. Process., 4: 304-305.
5. Grassel, Kathy (2002) "Taking out the Jack issues of Jetty Jack Removal in Bosque and River Taking out the Jack Issue of Jetty Jack Removal" in water Resources Program, The University of new Maxico, 1-46
6. Kalita S. (2017), "A Comprehensive Study on the Sediment Trapping Efficiencies of Various Riparian and Aquatic Vegetations on Open Channel flow Environment". HYDRO-2017, the 22nd International conference on Hydraulics, Water Resources and Coastal Engineering. L.D. College of Engineering, Ahmedabad.
7. Nicholas A.P. (2003), "Modelling and Monitoring Flow and Suspended Sediment Transport in Lowland River Flood Plain Environments". Erosion and Sediment Transport Measurement in Rivers: Technological and Methodological Advances.
8. Punmia B.C., Jain A.K. and Jain A.K. (2011), "Soil Mechanics and Foundations". LAXMI PUBLICATIONS (P). LTD.
9. Rijn, L. C. V. (1984). "Sediment transport, part II: suspended load transport". Journal of hydraulic engineering, 110(11), 1613-1641.
10. Sharma N. and Nayak A. (2015), "RCC Jack Jetty and Bamboo Submerged Vanes Application for Navigation Fairway in Ganga River of India". SMART RIVERS 2015, Paper 173, Buenos Aires, Argentina, 7-11 September, 2015.
11. Singh B. and Goswami R.K. (2012), "Anthropogenic Influence on Flow and sediment regime of a River Basin". International Journal of Engineering Science and Technology".

12. Sinha T. (2017), “Effect on Permeable Spurs (Porcupines) and their Dimensional Variations on the Erosion/Sedimentation Pattern of Open Channel Flow”. HYDRO-2017, the 22nd International conference on Hydraulics, Water Resources and Coastal Engineering. L.D. College of Engineering, Ahmedabad.